ADDIS ABABA UNIVERSITY
SCHOOL OF GRADUATE STUDIES
ADDIS ABABA INSTITUTE OF THECHNOLOGY
ELECTRICAL AND COMPUTER ENGINEERING DEPARTMENT

Radio Spectrum Sensing Comparative Analysis for Multiple Primary User Transmitter Detection

By: Ngist Fentie

Advisor: Prof. Mohammed Abdo

A Thesis Submitted to the School of Graduate Studies of Addis Ababa University in Partial Fulfillment of
Master of Science in Communication Engineering

July 12, 2021

Addis Ababa, Ethiopia

Addis Ababa University

Addis Ababa Institute of Technology

School of Electrical and Computer Engineering

Radio Spectrum Sensing Comparative Analysis for Multiple Primary User Transmitter Detection

By: Ngist Fentie

Approval by Board of Examiners

Dr. Bisrat Derebssa	_____
Dean, School of Electrical & Computer Engineering	Signature
Prof. Mohammed Abdo	_____
Advisor	Signature
Dr.Murad Ridwan	_____
Examiner	Signature
Dr. Yihenew Wondie	_____
Examiner	Signature

Abstract

A radio spectrum is a particular range of frequencies used to communicate information in a wireless communication system. It is naturally available and scarce resource. Besides to, the dramatically increase of the wireless communication system is a critical issue and the studies show that a certain licensed spectrum are underutilized. To solve this problem the cognitive radio is a key technology when there is a free spectrum band of the licensed users then the cognitive radio system permits that band for unlicensed or secondary users. In addition to that the cognitive radio system continuously monitors at the range of primary user transmission to minimize the interference by the secondary user's whole opportunistically occupies on the licensed bands. For this task the cognitive radio uses different spectrum sensing methods to avoid the undesirable interfering and recognize the accessible radio spectrum band for secondary users (SUs).

In this thesis, the performance of the Spherical and John's detector spectrum sensing methods in the presence of one and two primary users by implementing it over the typical Rayleigh fading channel is investigated. The performance of probability of detection and Receiver Operating Characteristics (ROC) curves within low signal-to-noise ratio (SNR) range is compared. Using the MATLAB software with the Monte Carlo techniques are used to evaluate and analysis of the performance of this work.

The implementation part shows a detailed comparison between the Spherical detector (SD) using General Likelihood Ratio Test (GLRT) estimator and John's detector (JD) using Locally Best Invariant Test (LBIT) estimator including a single and two primary user (PU) transmitted signals of detection. The specific, result shows the performance efficiency of detection for both schemes with a tolerable interference level under the fading channel.

The proposed system uses GLRT estimator for SD and LBIT estimator for JD. After doing the experiment, the result showed that JD provided the better detection performance over SD. To illustrate this, when two PUs are detected by four SUs in cooperative scheme using SD method at SNR range of [-2, -1] dB, the result is found to be incremented from 99.7% to 99.8%. The same experiment is done using JD method and the result shows that the detection performance is in the range of 99.9% and 100%.

KEY*WORDS: Spectrum Sensing, Spherical Detector, John's Detector, Rayleigh Fading Channel, Low SNR.*

Statement of Authorship

I, declare that this thesis is my exceptional work, has not been submitted to obtain a degree in this or other institutions. I further declare that all sources I used as reference have been acknowledged.

Ngist Fentie _____ _____

Name Signature

Place: Addis Ababa

Date of submission: July 12, 2021

This thesis has been submitted for examination with my approval.

Prof. Mohammed Abdo _____

Advisor's name Signature

Acknowledgements

First of all, I would like to thank the Almighty God for his unconditional love.

I would like to express my deepest thankfulness to my adviser Prof. Mohammed Abdo, for his insight that has led to the completion of this thesis. His guidance helped me in all the time of research and writing of this thesis.

I take this chance to honestly thank all the instructors of SECE who have been a source of knowledge. Finally, I would like to express my heart-full thanks to my friends who helped me for effective achievement of the thesis specially Tamirat Assefa and my beloved families for their wishes and bless.

Table of Contents

List of Figures

List of Tables

List of Abbreviations

AWGN	Additive White Gaussian Noise
BTS	Base-Station Transceiver System
BPF	Band Pass filter
CAF	Cyclic Auto Correlation Function
CDF	Cumulative Density Function
CR	Cognitive Radio
CRN	Cognitive Radio Network
CSF	Cyclic Spectral Density Function
DSA	Dynamic Spectrum Access
ED	Energy Detection
ETA	Ethiopia Telecommunication Agency
FC	Fusion Center
FCC	Federal Communication Commission
FSA	Fixed Spectrum Allocation
GLRT	Generalized Likelihood Ratio Test
IEEE	Institute of Electrical and Electronics Engineers
JD	John's Detector
LBIT	Locally Best Invariant Test
MAC	Media Access Control
MInT	Ministry of Innovation and Technology
MLRT	Maximum Likelihood Ratio Test
P_D	Probability of Detection
PDF	Probability Distribution Function
P_{FA}	Probability of False Alarm
PUs	Primary Users
QoS	Quality of Service
RAN	Radio Access Network
RF	Radio Frequency
ROC	Receiver Operating Characteristics
Rx	Receiver
SC	Selection Combining

SD	Spherical Detector
SECE	School of Electrical and Computer Engineering
SNR	Signal to Noise Ratio
ST	Spherical Test
SUs	Secondary Users
T_{SJD}	Test Statistics of John's Detector
T_{SMFD}	Test Statistics of Matched Filter Detection
T_{STD}	Test Statistics of Spherical Detection
TV	Television
Tx	Transmitter
WRAN	Wireless regional Area Network
xG	Next Generation

Chapter 1: Introduction

1.1 Over View

From the starting of wireless communications, the radio spectrum was one of the key components of the wireless communication system. Besides to that spectrum is a limited and valued natural resource. So that the use of available radio spectrum has been frequently a matter of concern. In addition to that, a static spectrum allocation policy adopted by governments of many countries has caused underutilization of spectrum because a huge segment of licensed radio spectrum is not efficiently used [1]. Conventionally, a licensed spectrum is allocated over comparatively long periods and is likely to be used first by licensed users [2]. The allocation of spectrum band to operators is the responsibility of a government organization. This activity in Ethiopia is handled by the Ministry of Innovation and Technology (MInT); in the USA by the Federal Communications Commission (FCC). This method is called the fixed spectrum allocation (FSA) arrangement and with this, the radio spectrum is divided into bands allocated to distinct technology-based services, e.g. mobile telephony, radio, and TV broadcast services. The FSA supervision structure guarantees that the radio frequency spectrum is entirely licensed to primary users (PUs) without interference [3].

Now the fast-growing of wireless communication has increased the difficulty of spectrum utilization and made it more challenging. On the hand, the rising diversity (voice, short message, Web, and multimedia) and demand for high quality-of-service (QoS) applications have resulted in overcrowding of the allocated spectrum bands leading to minimized levels of customer satisfaction.

The challenge is mainly serious in communication-intensive circumstances such as in the case of people crowds. On the other hand, the major licensed bands which allocated for television broadcasting are grossly underutilized which resulting in spectrum excess. For example, studies from the Federal Communication Commission (FCC) show that the utilization of licensed spectrum only ranges from 15% to 85% [4]. The national radio frequency spectrum allocation table prepared by the Ethiopian Telecommunication Agency (ETA) shows that the spectrum in the 960M–3GHz band as highly underutilized [5,6]. This creates an opportunity for cognitive radio to open licensed bands to unlicensed users. This is known as the dynamic spectrum access (DSA). Accordingly, the IEEE has formed a working

group IEEE 802.22 to develop an air interface for opportunistic secondary access or dynamic spectrum access DSA via cognitive radio technology [7].

Cognitive radio (CR) is a new idea that was 1st proposed by J. Mitola and Gerald Maguire [1] and was offered as an additional of software-defined radio enhancing flexibility of personal wireless services with the radio domain model and computational intelligence. Therefore, CR is an exciting and new way of thinking about wireless communications. Finally, it is already being considered as one of the main candidate technologies for the fifth-generation wireless systems which aim to give a higher data rate transmission, enough capacity, cost efficiency, and very sophisticated services.

CR aims to improve the spectrum utilization and efficiency of spectrum usage by opportunistically accessing the licensed spectrum without interfering with the licensed users [8]. To avoid using the spectrum at the same time with the licensed users, CR has to determine the existence of the primary user (PU) by sensing the spectrum band. It can communicate to its receiver if the spectrum is vacant. However, when the primary transmitters retransmit again, the CR transmitters should be stopping their transmission immediately to avoid creating interference to the PUs. Hence, spectrum sensing is a vital for CR system.

Using spectrum sensing the CR system can be granted the existence of PU's and communicate to utilize the spectrum band for secondary users. There are many types of spectrum sensing methods such as Energy detection, Matched filter detection, Cyclostationary feature detection; Eigenvalue based detection, Spherical detection, John's detection, Interference-based detection, Centralized, Decentralized, and Relay assisted detections. However, except Eigenvalue based, Spherical, and John's detection, all of these are used for single primary user transmitter detection. In the future, a single primary user spectrum sensing scenario of CR networks may fail due to the increasing of traffic congestion in different services. This thesis focuses on dealing with the performance comparison between Spherical and John's detector which are optimal detection schemes for multiple primary user spectrum sensing over multipath Rayleigh fading channel with low SNR range.

1.2 Statement of the Problem

The increasing demand of wireless communication leads to the scarcity of frequency spectra and the available radio spectrum is a limited natural resource, being overfilled day by day. To solve the scarcity of radio spectrum, Cognitive Radio Technology is a promising technique with spectrum sensing using non-cooperative and cooperative scheme in a wireless communication system provides high spectral efficiency.

However, in case of non-cooperative scheme due to the hidden node problem the primary user is not completely free from the interference affected by secondary users. To solve this problem cooperative spectrum sensing with a single primary user (licensed) band is considered as a solution to increase the detection performance, but the spectrum sensing using a single primary user leads to analytically controllable problem and increases the traffic congestion.

For this reason, this thesis explores to a way for accurate spectrum sensing of multiple transmitters of primary user with multiple secondary users in cooperative detection to provide better detection performance, with minimum traffic congestion for primary users.

1.3 Objectives

1.3.1 General Objective

- The main objective of this thesis is to do the analysis of a consistent radio spectrum sensing in the presence of multiple primary user transmitter that detects by multiple secondary users in the range of low SNR to provide the better detection performance under the Rayleigh fading channel.

1.3.2 Specific Objectives

This thesis specifically aims to achieve the following specific objectives:

- To investigate the techniques that uses to improve the spectrum sensing for multiple primary user transmitter detection methods such as spherical and John's detector.
- To study the behaviour of Spherical detector using GLRT and John's detector using LBIT estimator under single and multiple primary user transmitter detectors.
- To investigate the performance efficiency of both detectors under the Rayleigh fading channel.

- To perform the simulation for each technique and study the results by comparing their performance.

1.4 Literature Review

Various studies have been made on the area of spectrum sensing techniques within different methods in the cognitive radio technology; from those the following are reviewed as a frame scope of the thesis and existing challenges.

In the idea, of multiple primary user (PU) spectrum, sensing is to find primary transmitters working at a specified time by spending local measurements and interpretations with minimum traffic congestion for primary users (PUs). With the help of a Spherical and John's detection method, the cognitive radio transmitters observe the presence or absence of the primary signal based on the test statistics of the population covariance matrix of the received signal from primary transmitters.

In [9] the response of conventional energy detection (ED) by insertion of the adaptive Wiener filter on the front end of ED has been analysed under AWGN and Rayleigh fading channels. In this work, all the spectrum sensing performance metrics are improved. Moreover, at lower value of signal-to-noise ratio (SNR) range the performance of the energy detector has improved that compared to high SNR. However, this work is concerned only based on the single primary user detection method.

In [10] the work was based on the estimated value of the received PU signal SNR to determine the type of detection scheme. If the received signal SNR value at SU is strong enough the system will use a non-cooperative scheme. However, the received signal SNR is very low the SUs will detect with cooperatively each other to determine the presence or absence of the PU signal by sending their sensing information to the fusion center (FC). This work contributes to achieve the good detection performance without causing interference to PU with reduced complexity, low sensing time, and less traffic overhead. Because of it uses adaptively the combination of cooperative and non-cooperative ED detection it also improves the bandwidth efficiency. However, this work is concerned only based on a single PUs which detected by using more than two SUs. The proposed approaches in the consideration of more than one PUs which detected by cooperatively scheme of secondary users and evaluating its performance at low SNR.

The work in [11] investigated the sensing performance of multiple primary user detection under AWNG channel, based on the Spherical test (ST) detector. In this paper, some performance can be obtained via the Spherical test detector with information of non-blindly about the primary users. In addition to that the analytical formulae have been derived for the key performance metrics of the ST detector. The performance gain over several detection algorithms are observed in these works with noise uncertainty and a large number of primary users under AWGN channel. The proposed method is using the Rayleigh fading channel without requiring prior information (blindly) of the primary users.

In [12] the study shows the derivation of asymptotic threshold calculation for ST and John's detectors (JD) and the effect of noise correlation on the performance of the Rayleigh fading channel. In this paper, an asymptotic analysis was presented for ST and JD detectors only under the noise correlation hypothesis. The proposed method approaches for both detectors to evaluate the performance under uncorrelated noise and correlated signal with non-central complex Wishart distribution at low SNR which is not practiced in the open literature under Rayleigh fading channel.

In this thesis work the performance comparisons between the Spherical and John's detection methods over a Rayleigh fading channel with the presence of one and more than one primary user is to be investigated. In addition to that for increase the detection performance, the investigation is using cooperative sensing scheme of secondary users. The design of the detector satisfies the fundamental sensing requirements proposed in IEEE 802.22 WRAN (false alarm probabilities ≤ 0.1) [6].

1.5 Thesis Contribution

Due to technological development as well as the increasing network size arising from wireless communication service demand, the spectrum scarcity is one of the most challenging tasks in the telecommunication industry. Therefore, a unique attention is given to the cognitive radio network and its spectrum sensing performance.

This study contributes to giving information that is advantageous to minimize the interference caused by multiple secondary users when it uses more than one licensed band opportunistically and reduces the primary user traffic congestion. It also supports to achieve the desired performance requirements before network deployment. It offers a detailed

consideration of the Spherical and John's detector over the Rayleigh fading channel environment which is important for a multipath channel.

1.6 Limitation of the Study

The research:

- Limited to depending on the theoretical analysis and the simulation-based investigation.
- Studies only with Rayleigh fading channel environments.

1.7 Organization of This Paper

The remaining parts of this thesis paper are well-organized as follows. Chapter 2 review the contextual studies of cognitive radio: network communication, its network architecture and fundamental cycles. Chapter 3 introduces spectrum sensing, system model & reviews spectrum sensing methods: Transmitter detection, cooperative detection, & interference-based detection and existing overview of single transmitter detectors: Energy detection, matched-filter, & Cyclostationary feature detection. Moreover, it discusses about multiple transmitter detection: Eigenvalue based, Spherical and John's detector. Some detailed descriptions are given about Spherical and John's detector which are preferred in this research. Chapter 4 describes the main part of theoretical analysis of this thesis work which is importance to performance analysis. The analysis includes measuring performance parameters such as SNR, conducting statistical test analysis and calculating the probability of detection (P_D) of the designed system and finding the probability of false alarm (P_{FA}). In addition, calculation of threshold is also done in this chapter. Furthermore, the aforementioned calculations are done for both Spherical & John's detector in cooperative spectrum sensing with selection combing scheme over Rayleigh fading channel. The next chapter, Chapter 5, deals with the detailed discussion of simulation results. This includes the comparative analysis of Spherical and John's detector in the presence of one and two PUs which detects by SUs in cooperative manner over Rayleigh fading channel. The interpretation of detection performances is analysed by using different parameters that include measuring the performance of the system on different SNR values, the effect on performance detection by varying the value of P_{FA}. And providing a detailed illustration of complementary ROC curves. In this section, performance comparison of John's detector with eigenvalue-based detector is also included. Finally, Chapter 6 presents the conclusion and recommendation about the future research direction of this thesis.

Chapter 2: Cognitive Radio

2.1 Introduction

Cognitive radio is an intelligent wireless communication system that is aware of its surrounding environment, and understands by constructing to learn from the environment and familiarize its internal states to statistical variations in the incoming RF stimuli by making corresponding variations in certain operating factors in real-time, with two primary aims in attention [13]:

- Highly reliable communications every time and everywhere required;
- Efficient use of the radio spectrum.

Furthermore, cognitive radio is a device which has ability to observing the external radio environment in order to orient them to the current situation and act accordingly to communicate with other devices while keeping the recommended quality standards [15].

In wireless communication the spectrum remains underutilized in the present circumstances [14]. For improve its utilization, cognitive radio is introduced dynamically utilize the spectrum holes (free bands). Figure 2.1 shows the concept of spectrum holes that are used dynamically by the secondary users when it is not occupied by PUs.

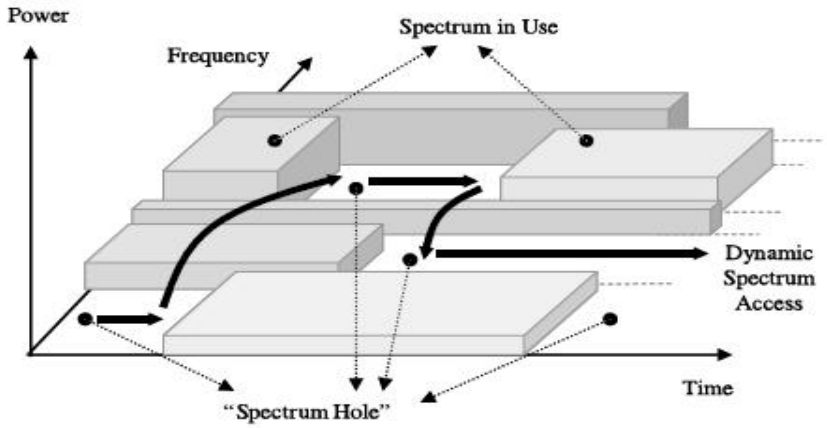

Figure 2.1: Dynamic access of the spectrum holes [22].

2.2 Cognitive Radio Network

A cognitive radio network (CRN) which contains more than one CR nodes, and similar to the conventional wireless networks, classified as either an infrastructure-based network or an ad-hoc network [17]. Every CR node might have a similar or dissimilar level of cognitive capability in a CRN. The CRN can be supposed as an intelligent overlay network with several coexisting networks, and each CR nodes might be belonging to different coexisting networks. From this, the CR nodes are likely to have different levels of cognitive capability [18].

For effectively utilization of spectrum in opportunistically manner the cognitive radio network is the efficient solution. Cognitive radio network (CRN) users are categorized as in two portions.

1. Primary users (PUs) that are licensed to use a limited part of the spectrum band.
2. Secondary or cognitive users (SUs) use the spectrum licensed to some primary user in dynamic manner.

The secondary user would search for “white-spaces” or “spectrum holes” in its vicinity and rapidly alter its transmission parameters according to the prevailing conditions such as:

1. When the selected channel is busy by primary users it detects the other vacant channel opportunistically.
2. Extract the information with regarding the presence of active PUs in a fixed frequency band and geographical location which is support and used to reduce the interference to the PUs [16].

Figure 2.2: Shown CRN which includes the following system components and tasks of each layers.

PHY Layer: A vital section in spectrum sensing that allows CR users to know the free spectrum bands, whereas environmental knowledge requirements to achieve the best level of radio environment awareness, such as the channel-state information or channel gain from the CR Tx to the primary Rx.

MAC Layer: Used to the CR to perform with spectrum sensing scheduling, spectrum-aware and sensing-access coordinator [18]. Each part preforms its function as follows:

- **Spectrum Sensing Scheduler:** Controls the sensing operations.

- **Spectrum Aware MAC:** Used as regulator for spectrum access to the recognized spectrum holes.
- **Sensing-Access Coordinator:** Controls the operations of the above two functions in a time basis by taking care of the interchange between the sensing requirement and the spectrum access opportunity that the CR user might be attain [18].

Network-Layer: Used to perform routing and statistical control. In this layer there are three significant tasks are:

- **Network Tomography:** It is a type of statistically measuring, processing, and inferring methods that provide the parameters and traffic/interference patterns for CRN operations at both the link and network levels [19].

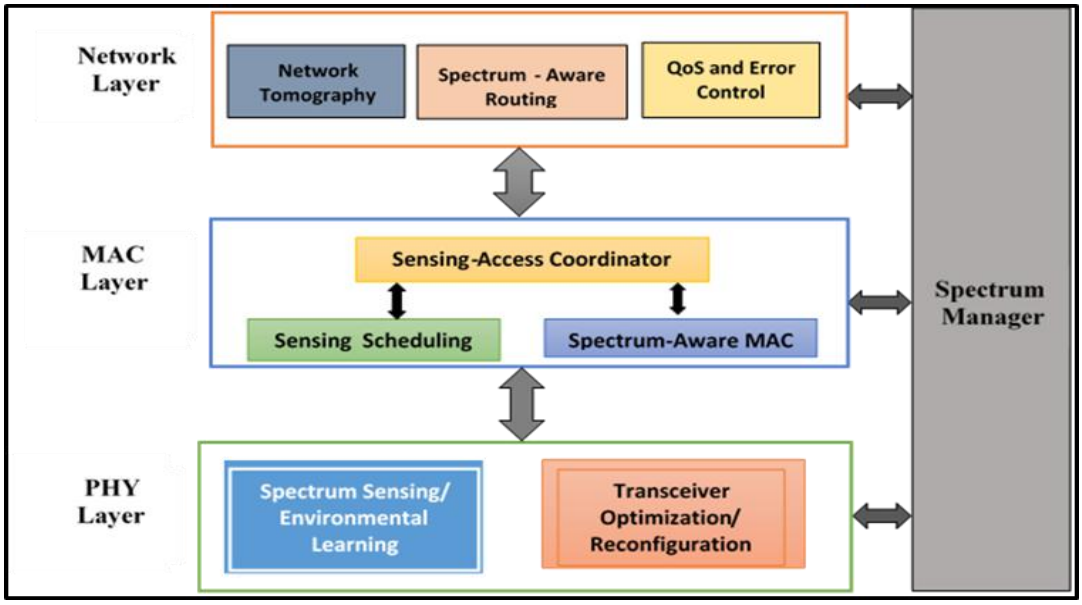

Figure 2.2: The key tasks of the PHY, MAC and network layers in a CRN [18].

- **Quality of Service (QoS) and Error Control:** It controls the level of standardized tolerable **QoS** performance values based on IEEE and used to govern the error in CRN communication system.
- **Spectrum Aware Routing**: A direction-finding protocol which exploits the local spectrum heterogeneity and allocates dissimilar channels to links on the similar stream to minimize the interference.

Spectrum Manager: It provisions the access of vacant spectrum in a dynamic and effective manner by interconnected each three layers.

2.3 Cognitive Radio Network Communication

Cognitive radio network communication is the way of information exchange between the primary transceiver and the cognitive radio transceiver. Therefore, it is the basic principles of spectrum sensing that could safeguard the PUs from the interference [18]. As indicated in Figure 2.3 primary transceiver (Tx and Rx) with cognitive radio transceiver (CR Tx and Rx). In this process a primary Tx sends data to its intended Rx in a certain licensed frequency band. On the other hand, a pair of CR users (Tx and Rx) intends to access the free bands for secondary communication. The CR Tx requires executing spectrum sensing to find spectrum holes and guarantee the protection of PUs. Mainly CR Tx needed to detect to check the existence of an active primary receiver inside its coverage. If not, the CR Tx can safely transmit to the CR Rx using the identified spectrum hole. Otherwise, the CR users are not allowed to use the band. Thus, detecting the nearby primary Rx's can directly identify the spectrum hole, which is called direct spectrum sensing [20].

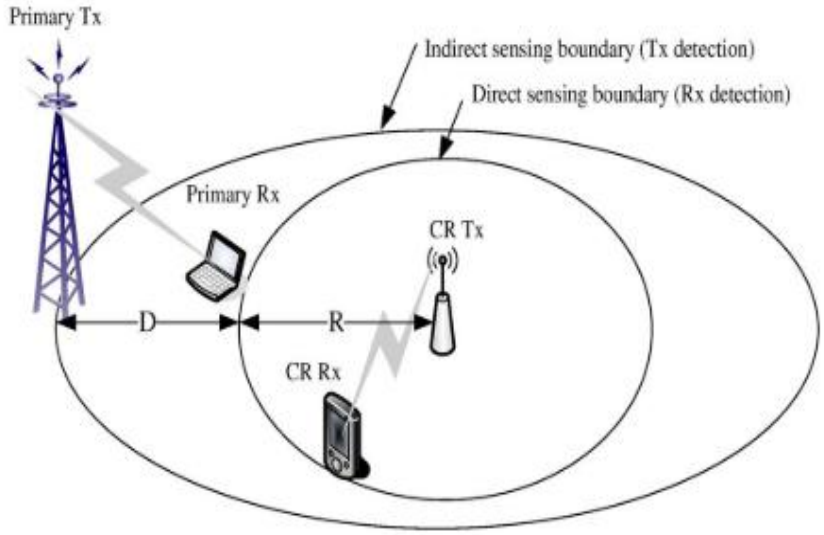

Figure 2.3: "Principles of spectrum sensing" [18].

Most of the existing spectrum sensing schemes are identifies the spectrum holes by detecting the primary Tx's [21] [22]. Depending on the transmission distance ranges the spectrum sensing categorized as indirect and direct sensing.

1. Indirect sensing is requiring a very week licensed signal. This method increases the spectrum sensing has been more challenging. Compared to the direct spectrum sensing, indirect spectrum sensing requires a greater detection range as shown in

Figure 2.3 from R to R+D and the signal-to-noise ratio (SNR) of the primary signal is low enough below the SNR wall [23]. It is impossible for the CR Tx to detect the primary Tx, even if the infinity number of samples of the primary signals are used. For example, in Figure 2.3, the transmission range between the primary transceiver is the interfering range of the CR transmitter. In this range, the CR Tx needs to detect the presence of an active primary Tx within a distance range of D +R. If the distance between the primary and the CR Tx's is greater than D+R, there will be no active primary Rx inside the interfering range of the CR Tx, and then, the CR Tx can safely access the spectrum bands [20].

2. Direct sensing is the most effective way of spectrum sensing to detect directly the primary Rx. Because, it is the receiver of a primary user system that should be protected.

2.4 Cognitive Radio (xG) Network Architecture

Cognitive radio is the vital supporting technology of xG network which delivers the capability to use or share the spectrum in an opportunistic way [22]. For the development of communication protocols, a perfect explanation of the xG network architecture is a fundamental issue [22]. The main parts of the xG network architecture are as shown in Figure 2.4 can be classified in two groups as the primary network and the xG network (secondary networks) [23].

- **Primary Network:** It has the prevailing network infrastructure with an exclusive right to access an assured spectrum band. For example, the common cellular and TV broadcast networks. The primary networks have the following sub parts:

- **Primary User (PU):** It has a permission to work in a definite spectrum band. It is well-ordered by the primary base station and it should not be affected by any operations of secondary users.

- **Primary Base-Station:** Also, know as licensed or primary base-station which has a permanent infrastructure network with the spectrum licenses such as a base-station transceiver (BTS) in a cellular system [35].

- **NeXt-Generation (xG) Network:** It is a DSA or SUs network which does not have a permission to operate in the desired licensed band. Therefore, the spectrum access is

permitted only an opportunistic way. NeXt-Generation networks can be deployed both as an infrastructure network and an ad-hoc network as shown in Figure 2.3.

- **NeXt-Generation Users:** Those are unlicensed users (CR users or SUs) which are no spectrum licensed to use it. Hence it should be performed additional functionalities to share the licensed spectrum bands.
- **NeXt-Generation Base-Station:** Also known as unlicensed or secondary base-station with a fixed infrastructure component and cognitive radio capabilities. It provides the single-hop connection to xG users without licensed spectrum access

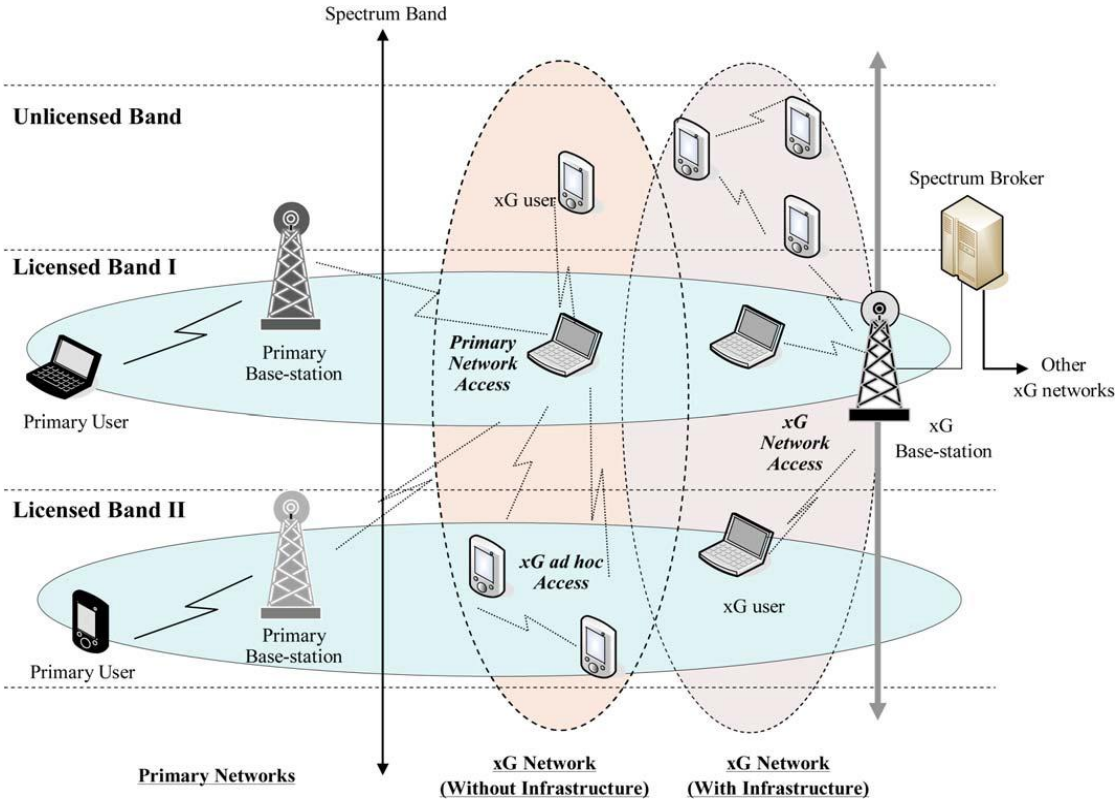

Figure 2.4: Cognitive radio (xG) network architecture [23].

- **Spectrum Broker:** It is a central network unit that plays a role in sharing the spectrum resources among various xG networks. It also can be linked to each network and assist as a spectrum information director to allow the coexistence of several xG networks.

2.5 Cognitive Radio Cycle

The sequence of operations in cognitive radio that are necessary to perform adaptive operation is called cognitive cycle [13]. The Figure 2.5 shows the basic cycle of cognitive radio and its component with descriptions [24] [25]-[28] as follows:

- **Spectrum Sensing:** It is one of the main duties of cognitive radio that used to detect the available portions of the spectrum. A cognitive radio monitors the free spectrum bands in the accessible frequency ranges, captures their information, estimates the interference temperature of the radio environment, and detect probable free channel by using the compatible detection techniques.

- **Spectrum Analysis**: It is the procedure that takes input about accessible free spectrum band from spectrum sensing block and achieves channel identification where in a number of parameters are evaluated and involves for each free band sensed by the spectrum sensing process.

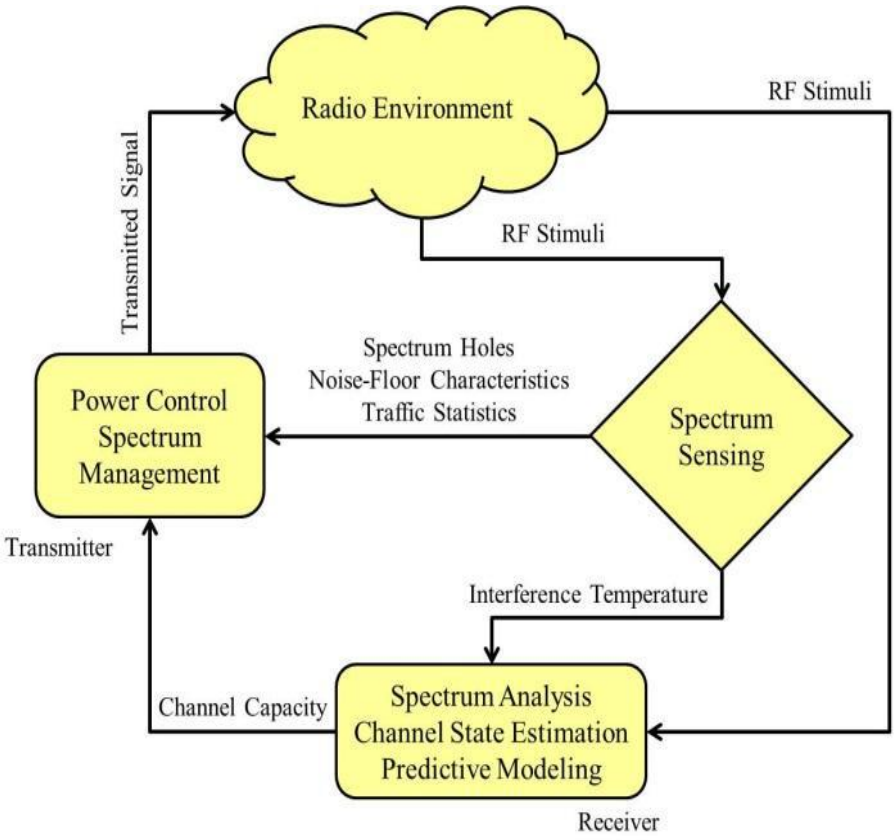

Figure 2.5: Fundamental cognitive cycle [24].

- **Spectrum Decision/Management**: The stage of the cognitive cycle while an actual decision regarding with the best accessible spectrum hole is taken on the origins of analysis done by the earlier two stages. Parameters like transmission mode, data rate, transmit power control and transmission bandwidths are taken into consideration here.

Chapter 3: Radio Spectrum Sensing

3.1 Introduction

Spectrum sensing is the duty of finding free spectrum bands by sensing the radio spectrum in the local neighbouring of the cognitive radio receiver in an informal way and a very task of the perfect cognitive radio procedure breakdowns [29]. Particularly it performs in cognitive radio such activities as detection of free bands, identification of the spatial directions of incoming interferes, the spectral determination of each spectrum situations, and signal classifications.

In this scenario, cognitive radio uses spectrum sensing mainly to avoid unsafe interfering with primary users (licensed users) and detect the vacant spectrum to refine the spectrum exploitation. Underutilization of the radio frequency band had resulted in the spectrum holes or white spaces which will provide an opportunity for the users without a license to use it [30]. Based on the occupancy and interference level, the radio frequency spectrum can be divided as a black space that is fully occupied; grey space that is partially occupied; white space that is not occupied and have low interference level with the only interference being noise.

Spectrum holes are separate as the spectrum bands that can be used by the unlicensed users (SUs) dynamically without creating interference to the licensed users (PUs) [10]. This method of finding or detection of the spectrum hole is known as spectrum sensing [22].

3.2 System Model

The system model in Figure 3.1 shows how to interpret the spectrum hole by cognitive radio users (SUs). Initially, the received PU signal is estimated using General Likelihood Ratio Test (GLRT) or Maximum likelihood Ratio Test (MLR) for Spherical detector and Locally Best Invariant Test (LBIT) for John's detector. Then apply Spherical and John's detector equally with a cooperative detection scheme. Then with the help of soft-fusion center (FC) of selection combining (SC) scheme made the decision depending on the selected frequency bands either the presence of primary signal which is hypothesis (H_1) or absence of primary signal with hypothesis (H_0).

Finally, SUs can be accessing the free band (channel) if it is free otherwise continuous the sensing process until it gets the free band.

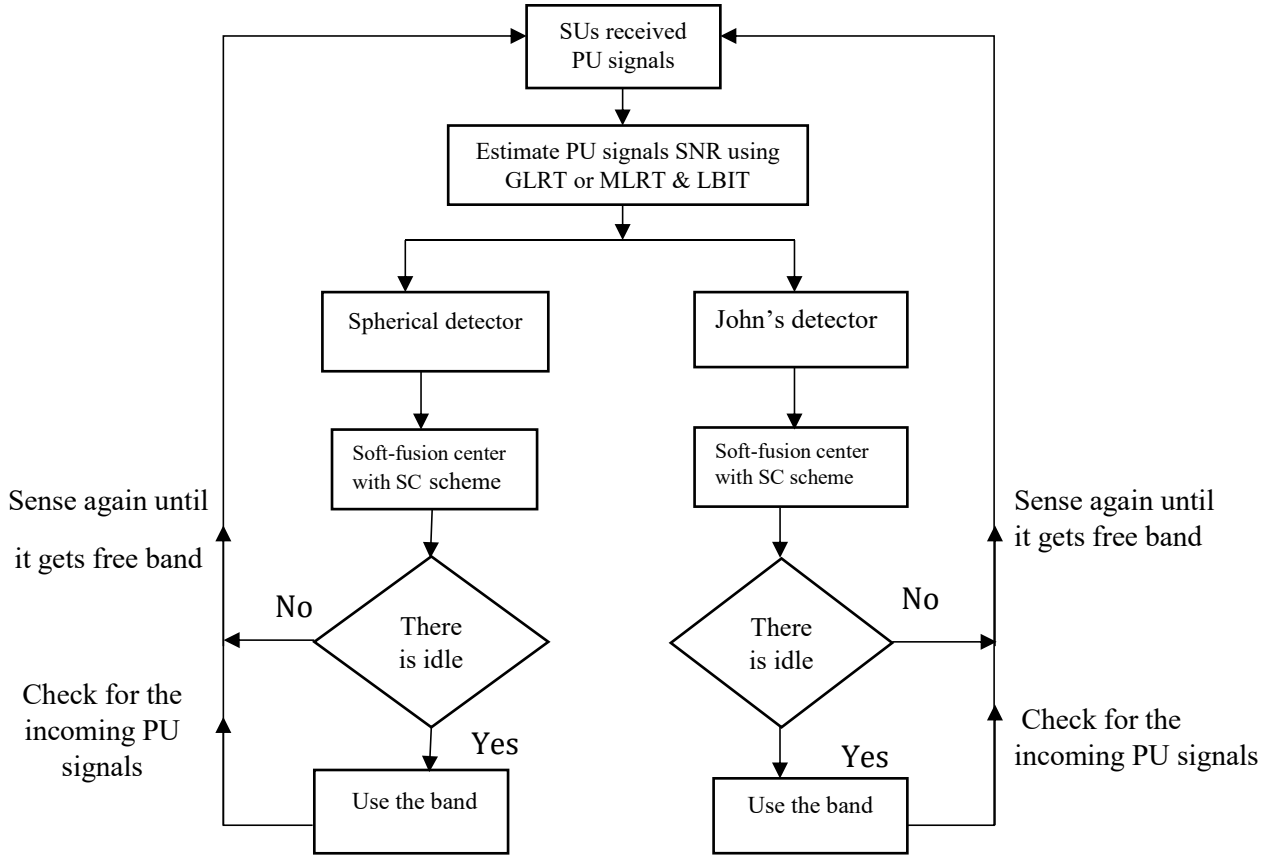

Figure 3.1: System model of both detectors.

All the time spectrum sensing aims to accomplish the accurate detection of received signals. But, due to the statistical nature of the problem, it is impossible in practice. From this, the signal detector intended to work within the minimum error level.

For spectrum sensing the performance indicators are the probability of detection (P_D) and probability of false alarm (P_{FA}) are the key parameters. Probability of detection is the correct declaration of the presence of the PUs (hypothesis H_1). In spectrum sensing methods most of the time the performance was affected by P_{FA} (hypothesis H_0). So, that P_{FA} is an interesting issue. For the better improvement of performance, the P_D must be maximized, and the P_{FA} rate to be kept as low as possible to allows system achievement transmissions with minimum interference level.

To identifies the required signal from noise in a single and multiple primary user with cooperatively sensing can be written as mathematically [31] in eq. (3.1) & (3.2).

$$x[n] = \eta[n] \qquad H_0 \qquad (3.1)$$

$$x[n] = hs[n] + \eta[n] \qquad H_1 \qquad (3.2)$$

Where $n = 1,2, \ldots, N$ number of discrete samples at receiver, $X[n]$ received signal with n samples, $\eta[n]$ is the AWGN with zero main and variance of ∂_η^2, h is the channel gain quantity and $s[n]$ is the signals which comes from primary transmitter. The hypothesis H_0 is only noise sample and H_1 is transmitted signal pulse noise sample. In vector form the above (3.1) & (3.2) can be expressed as [31] in eq. (3.3);

$$x = \begin{cases} \eta & H_0 \\ \text{Hs} + \eta & H_1 \end{cases} \qquad (3.3)$$

Where, $x \in C^{KP \times N}$ is a dimensional complex vector, which represents the receiving data vector to sense P PUs, the $K \times 1$ vector η is the additive complex Gaussian noise vector with having zero mean and covariance matrix of $\partial_\eta^2 I_K$, H is the $K \times P$ dimensional matrix coefficients of the channel gain and s is the $P \times 1$ matrix of the primary transmitter signal vector.

3.3 Methods of Radio Spectrum Sensing

Depending on the requirement of cognitive radio; there are so many classification approaches in spectrum sensing methods [32]. Among these, some are listed below based on the signal estimation and need to detect.

1. Frequency domain approach (direct method): The estimation takes place directly from the signal.
2. Time-domain approach: The estimation is performed using the autocorrelation of the signal.

On the other hand, based on the necessity of spectrum sensing there are different classifications of spectrum detection methods have been described to identify the presence or absence of signal transmissions in the surrounding environment [15] as shown in Figure 3.2 generally categorized as:

- Cooperative Detection;
- Non-Cooperative Detection (Transmitter Detection);

- Interference Based Detection.

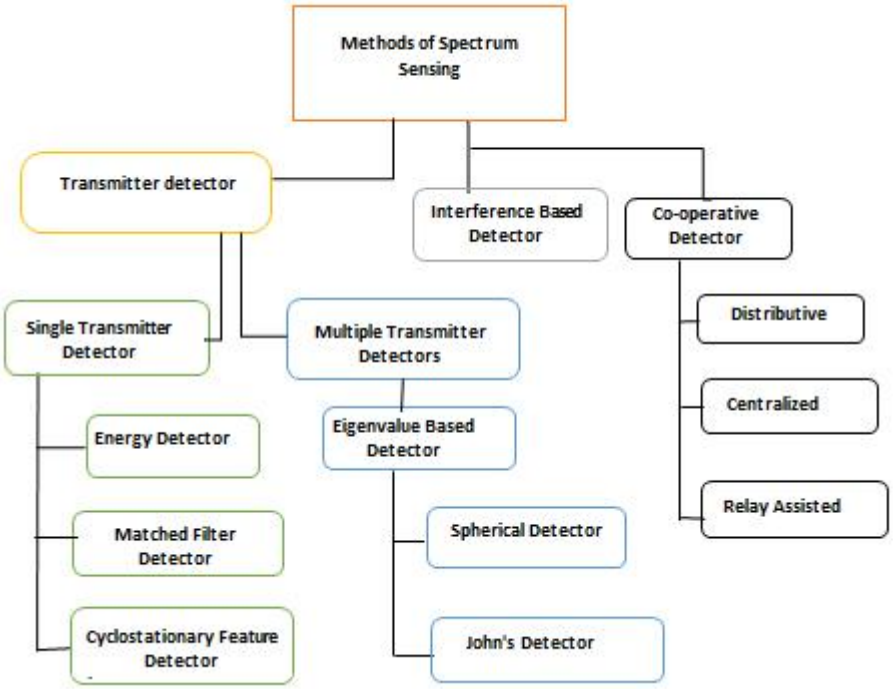

Figure 3.2: Spectrum sensing methods [32].

3.4 Single Primary Transmitter Detection

It is the detection of a frequency band of primary user which comes from a single primary transmitter. In this scenario the detector is perform the sensing tasks based on the received SNR comes from primary transmitter. And the detector can be decide whether the present or absence of PU [33]. This transmitter detector includes the blind spectrum sensing these are energy and eigenvalue-based detection, and the non-blind spectrum sensing are matched filter and Cyclostationary feature detection. Both of blind and non-blind spectrum sensing methods are can be detecting a free spectrum band by using local sensing method (non-cooperatively) which is a simple and requires low processing times, each SU seeks for its aims and does not take into account the decisions of other SUs [22]. So, it performs their sensing task without information exchange between SUs.

3.4.1 Energy Detection

This is mostly used spectrum sensing techniques which works without the need for prior information of primary user signal. It also performs fine with unidentified dispersive channels. Energy detection has less computational, implementation complexity, and less delay relative

to the other methods [29]. Because of unknown prior knowledge of primary user transmitted signal properties depend on the information of accurate noise power. Hence it is vulnerable to noise uncertainty. In high SNR situations, it is an optimal detector for detecting independent and identical distribution signals. In this method, the decision is based on the received signal energy with a specified frequency band compared to the threshold value. If the received signal energy is larger than the threshold value then the spectrum band is working by PU. On the other hand, the received signal energy is less than the threshold value then it is important there is a spectrum hole.

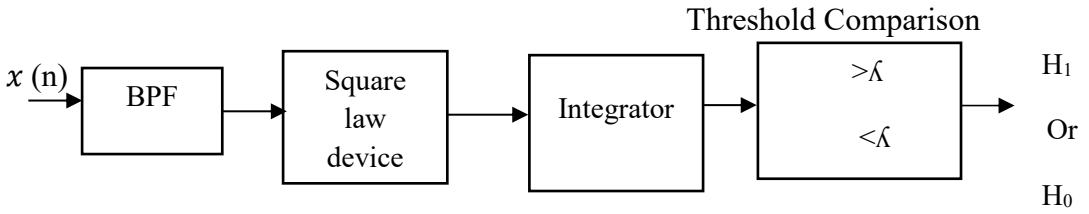

Figure 3.3: Block diagram of energy detection [20].

As indicated in Figure 3.3 the received signal is passed through the bandpass filter which selects the specific band of frequency to sense and then through a square-law device to calculate its energy. The average energy of the signal is calculated by integrating it over an observation time interval through an integrator [20]. The output energy from the integrator block is then compared to a pre-defined threshold that used to determine the presence or absence of the primary user. The mathematical model of energy detection is as follow with a primary signal received at cognitive radio plus noise [34]:

$$Y[n] = X[n] + \eta[n] \tag{3.4}$$

Where $n = 1, 2, 3, ..., N$ sample intervals, $Y[n]$ received sample signal, $X[n]$ is the transmitted sample signal by the primary transmitter and $\eta[n]$ is the additive white Gaussian noise.

The performance of energy detection evaluated by the detection probability(P_D) and P_{FA}. The "probability of primary user detection" and the "probability of false detection" methods can be calculated within the specified threshold value λ[10]:

3.4.2 Matched Filter Detection

This is a coherent sensing technique and requires accurate knowledge of the transmitted signal from the PU to optimally detect the signal at the cognitive user [35]. That means it

involves with the perfect knowledge of the primary signalling features such as bandwidth, operating frequency, modulation type, pulse shaping, and frame format [32]. That awareness's are used to it to demodulate the received primary signal at CR receiver. Because of it has been prior knowledge of transmitted signal information at the receiver it needs the lowest detection time.

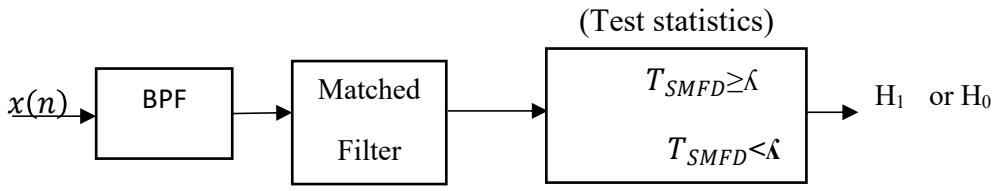

Figure 3.4: Block diagram of matched filter detection [20] [35].

At the beginning, "the input signal passes through a band-pass filter; this will measure the energy around the related band, then the output signal of BPF is convolved with the matched filter whose impulse response is similar to the reference signal" [32][36]. Finally, the matched filter output value is compared to a threshold value for detecting the existence or absence of the primary user. The operation of matched filter detection is expressed as in mathematical [32] [35] in eq. (3.5).

$$Y[n] = \sum_{k=-\infty}^{\infty} h[n-k]X[k] \tag{3.5}$$

Where, $Y[n]$ is the output of the signal from BPF filter for the received signal and hence response $h[n] = S[N-1-n]$ for $n = 0, \ldots, N-1$, $X[k]$ is the unknown signal (vector) and it is convolved with the (h), the impulse response of a matched filter is matched to the reference signal for maximizing the SNR [32]. The decision of the presence or absence of licensed user is based the comparison of the test statistics T_{SMFD} with threshold value λ.

3.4.3 Cyclostationary Feature Detection

Cyclostationary feature detection method studies with the inherent Cyclostationary properties of the signals [37] that can't be found in any interference signal or stationary noise. These are the periodic statistics and spectral correlation. This periodicity exploits in the received primary signal to identify the presence of PUs.

Cyclostationary feature detection has ability to keeps the higher noise protection compared to any other spectrum sensing methods [37]. Because of its noise rejection capabilities, it can be

alleviate the influence of noise, and can be provide the better detection performance with low SNR.

For investigation of Cyclostationary feature detection the study of autocorrelation function is a vital issue. By considering the received signal $X(t)$ is a sine wave which satisfies all condition of Cyclostationary properties and periodic in time t [37][39]. Then the autocorrelation function $R_X(\mathrm{t}, \tau)$ can be calculated as with time offset τ [38] in eq. (3.6).

$$R_X(t, \tau) = R_X(\mathrm{t}+ T_0, \tau) \tag{3.6}$$

From (3.6) can be find the cyclic autocorrelation function (CAF) by using Fourier transform of autocorrelation function which is important to derive the cyclic spectral density function (CSF) which used to detect the PU signals [38] in eq. (3.7) & (3.8).

$$R_X{}^{\alpha}(\tau) = \frac{1}{T_0}\int_{T_0} R_X\,(t, \tau)e^{-j2\pi\alpha\tau}d\tau \tag{3.7}$$

$$S_X{}^{\alpha}(f) = \int_{-\infty}^{+\infty} R_X{}^{\alpha}(\tau)\, e^{-j2\pi f\tau}d\tau \tag{3.8}$$

Where α is cyclic frequency, so in this way, the SUs can be distinguishing Cyclostationary signal from noise by calculating CAF and CSF on different cyclic frequencies. Where $R_X{}^{\alpha}(\tau)$ is the CAF of continuous signal and α cyclic frequency and $S_X{}^{\alpha}(f)$ is the power spectrum of the signal for α = 0. The detection schemes search for peak cyclic spectrum magnitude of the signal at any of the cyclic spectrum magnitude of the signal at any of the cyclic frequencies [35]. If the peak is found then the signal is existing otherwise signal does not exist.

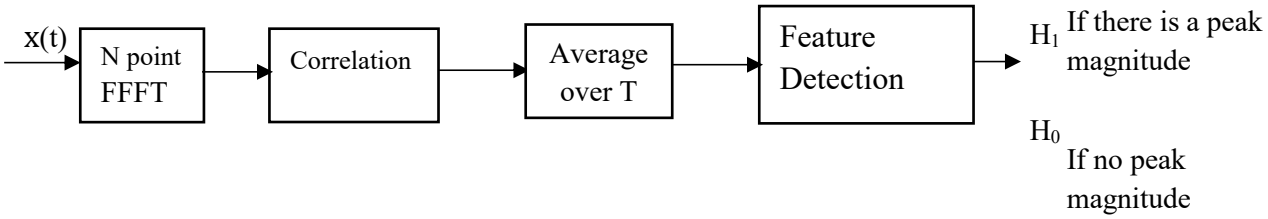

Figure 3.5 Block diagram of Cyclostationary feature detection [20] [34] [35].

The performances of the Cyclostationary feature detector also depend on signal energy. Because of it uses different modulation methods used to suffer to change the energy on the signal. Moreover, the technique will require coherence of signal information like carrier frequency and sensitive to sampling offset [35]. This will increase the detection time as compared to energy detection.

3.5 Multiple Primary User Transmitter Detection

This method of spectrum sensing is the process of detection spectrum holes in the presence of two or more than primary (licensed) transmitters which detected by the cognitive radio transmitter. In this process first, the cognitive radio transmitter perform detection to check whether or not the licensed band occupied by the primary users. This activity is an importance for guarantees the licensed users from interference and to find the spectrum holes. In this method the cognitive radio perform their tasks as the following ways: If the licensed user is occupied on the specified band or the spectral resolution then the cognitive radio transmitter does not transmit their information to the allocated secondary users. On the other hand if there is any free band then it can be access that band and transmits its required information to secondary users. Because of it uses more than one primary transmitter detection; the opportunity of secondary users to access the free band is better than compared to single primary transmitter detection. These methods also have a significance role to minimize the PU traffic congestion affected by SUs.

3.5.1 Eigenvalue Based Detection

Eigenvalue-based detection is a novel method which is based on the Eigenvalues of the sample covariance matrix of the received signal at the secondary users (SUs) [39]. It is a solution to noise uncertainty problem. Eigenvalue-based detector outperforms conventional detector especially in multiple primary user scenarios, where multiple antennas (or multiple cognitive users) are cooperatively employed to detect the free spectrum bands.

This method achieves both high P_D and low P_{FA} without requiring information of the primary transmitted signals, channel, and noise power as a priori [40]. Since the covariance matrix joins the correlations among the signal samples. That is the presence or absence of licensed or primary signal is decided depending on the sample covariance matrix of the received signals.

The secondary receiver has the ability to understand the presence or the absence of a primary signal based on the largest and the smallest eigenvalue of the received signal of covariance matrix [41]. Assume that the received signal is confirmed with multiple licensed users [42]. Then in mathematical form can be written as;

$$X(\mathrm{n}) = \sum_{j=1}^{P} \sum_{k=0}^{Nj} h(k)_j s_j(n-k) + \eta(n) \qquad (3.9)$$

Where P and $n = 0, 1, 2, \ldots, N$ are the number of licensed users and samples.
The sample covariance matrix can be written as in mathematical [42] form;

$$R_x(N_s) = \frac{1}{N} \sum_{N=L-1}^{L-2+N_s} (\hat{X}(n)\hat{X}^H(n)) \tag{3.10}$$

Then the statistical covariance matrix of the signal and the noise can be calculated as [42];

$$R_X = E(\hat{X}(n)\hat{X}^H(n)) \tag{3.11}$$

$$R_s = E(\hat{s}(n)\hat{s}^H(n)) \tag{3.12}$$

$$R_\eta = E(\hat{\eta}(n)\hat{\eta}^H(n)) \tag{3.13}$$

It can be related that $\hat{R}_s$ meets in probability in [42];

$$R_X = HR_sH^H + \sigma_\eta^2 I_{ML} \tag{3.14}$$

Where σ_η^2 is the noise power, and I is ML order of the identity matrix.
Let from (3.14) the eigenvalues of the R_X and HR_sH^H can be expressed as: $\lambda_{1(max)} \geq \lambda_2 \geq \ldots \geq \lambda_{ML(\min)}$ & $\rho_1 \geq \rho_2 \geq \ldots \geq \rho_{ML}$ respectively [42]. By using the ratio of maximum to minimum eigenvalues; obviously the eq. becomes when there is a signal:

$$\lambda_n = \rho_n + \partial_n^2 \tag{3.15}$$

When no signal $\hat{s}(n)$=0, then $R_s = 0$, from that $\lambda_{1(\max)} = \lambda_2 = \ldots = \lambda_{ML(\min)} = \partial_n^2$. Then the ratio of the maximum to minimum eigenvalue becomes for two hypotheses as follows respectively (3.16) & (3.17).

$$\lambda_{1(\max)} / \lambda_{ML(\min)} = 1 \quad \text{No primary signal is present } (H_0) \tag{3.16}$$

$$\lambda_{1(\max)} / \lambda_{ML(\min)} > 1 \quad \text{Primary signal is present } (H_1) \tag{3.17}$$

3.5.2 Spherical Detector

The Spherical detector (SD) is a blind detection scheme, which performs the spectrum sensing without any prior information with respect to the noise power, channel gains, signal power and the number of primary user signals [43]. It is a very efficient method of multiple primary user spectrum sensing. Moreover, the Spherical detector is an optimal detector in the

Generalized Likelihood Ratio Test (GLRT) sense when the covariance matrix of the received primary signals is positive definite [11]. The SD performs spectrum sensing by evaluating whether the population covariance matrix differs from a matrix proportional to the identity matrix [43].

Calculating the sample covariance matrix R and the population covariance matrix Σ of received signal gives the Sphericity test statistic which used to compare the predetermined threshold. This process is an importance to made the decision whether the presence or absence of primary users. The threshold value is calculated from the false alarm probability and its correctness is an important to determine the performance. By consider the following received signal vector to calculating the test statistics [31] in eq. (3.18);

$$x = \mathrm{Hs} + \eta \tag{3.18}$$

Where, $H = [h_1, h_2, \ldots, h_P]$ is the $K \times P$ dimensional matrix denotes as coefficients of the channel gain, h_1 denotes all channel vectors between the first primary user and all K sensors (SUs). From these for all h_P can be expressed as H matrix;

$$H = \begin{bmatrix} h_{1,1} & h_{1,2} \ldots . & h_{1,P} \\ \vdots & \ddots & \vdots \\ h_{K,1} & h_{K,2} \ldots & h_{K,P} \end{bmatrix} \tag{3.19}$$

A $P \times 1$ vector $S = [s_1, s_2, \ldots, s_P]^T$ denotes the P primary user signals. Where the primary user signal samples are independent and identical distribution with complex Gaussian distribution of zero mean, and ∂_s^2 variance $S \sim N(0, \partial_s^2)$ and uncorrelated with noise. The H matrix is assumed as constant during the sensing time. According to (3.18) & (3.19) the received observation is expressed as $K \times N$ data matrix X;

$$X = [x_1, x_2, \ldots, x_N] \tag{3.20}$$

In reality every vector of x_N in (3.20) represents one sample of all detected primary signals received by cognitive sensors as follow;

$$x_{K,1} = \begin{bmatrix} h_{1,1} & h_{1,2} \ldots . & h_{1,P} \\ \vdots & \ddots & \vdots \\ h_{K,1} & h_{K,2} \ldots & h_{K,P} \end{bmatrix} \times [s_1, s_2, \ldots, s_P]^T \times [\eta_1, \eta_2, \ldots, \eta_K]^T \tag{3.21}$$

In this case with in K sensors, so the first received sample ($N = 1$) of the observation vector equals the sum of all primary user signals which are filter by the channel plus the complex Gaussian additive noise as;

$$x_{K,1} = \begin{bmatrix} h_{1,1}s_1 + & h_{1,2}s_2 + \dots & + h_{1,P}s_P + \eta_1 \\ \vdots & \ddots & \vdots \\ h_{K,1}s_1 + & h_{K,2}s_2 + \dots & + h_{K,P}s_P + \eta_1 \end{bmatrix} \tag{3.22}$$

Hence, the received observation data of X matrix with $K \times N$ dimension;

$$\mathrm{X} = \begin{bmatrix} x_{1,1} & x_{1,2} \dots . & x_{1,N} \\ \vdots & \ddots & \vdots \\ x_{K,1} & x_{K,2} \dots & x_{K,N} \end{bmatrix} \tag{3.23}$$

From eq. (3.23) R denotes the K×K test statistics of the sample covariance matrix;

$$\mathrm{R} = XX^H \tag{3.24}$$

Here, $(\ .)^H$ denotes the Hermitian complex conjugate [44]. Without channel model assumption in the absence and presence of PUs; the sample covariance matrix R= XX^H follows uncorrelated and correlated non-central complex Wishart distribution R ~ $W_K(\mathrm{N},\ I_K)$ and R~ $W_K\ (\mathrm{N}, \Sigma)$ of the population covariance matrix Σ respectively as follows [44] in eq. (3.25);

$$\Sigma = \begin{cases} \frac{E[R]}{\mathrm{N}} = \partial_\eta^2 I_K & H_0 \\ \partial_\eta^2 I_K + \sum_{p=1}^{P} \vartheta_p h_p h_p^H & H_1 \end{cases} \tag{3.25}$$

Where $\sum_{p=1}^{P} \vartheta_p h_p h_p^H$ is a positive definite matrix.

Then test statistics of Spherical detector (T_{STD}) calculated by using General Likelihood Ratio Test (GLRT) criterion [43] and separate from a constant, with the help of the likelihood function of the data matrix X which written as;

$$\mathrm{L}\ (\mathrm{X}/\ \Sigma) = (|\Sigma|)^{-N} e^{tr(\frac{-R}{\Sigma})} \tag{3.26}$$

Where $|\Sigma|$ denotes as determinant of population covariance matrix. Then the likelihood ratio statistic represented by ρ written as [11];

$$\rho = \frac{sup_{\partial_\eta^2 > 0} \mathrm{L}(\mathrm{X}/\partial_\eta^2 I_K)}{sup_{\Sigma > 0} \mathrm{L}(\mathrm{X}/\ \Sigma)} \tag{3.27}$$

Using the maximum likelihood ratio test (MLRT) to estimates the ∂_{η}^{2} for H_0 and Σ for H_1 as follows [45] respectively;

$$\widehat{\partial_{\eta}^{2}} = \frac{tr(R)}{KN} \tag{3.28}$$

$$\widehat{\Sigma} = \frac{R}{N} \tag{3.29}$$

By substitute eq. (3.28) & (3.29) in to eq. (3.27) [32] can be obtain;

$$\rho^{1/N} = \frac{|\mathrm{R}|}{(\frac{1}{K}\mathrm{tr}(\mathrm{R}))^{K}} = \frac{\prod_{i=1}^{K}\lambda_i}{(\frac{1}{K}\sum_{i=1}^{K}\lambda_i)^{K}} = T_{STD}. \tag{3.30}$$

Where λ_i represents the eigenvalues of R and $tr(R)$ represent the trace of observed sample covariance matrix of R [45]. Finally, to make a decision whether the presence or absence of PU signal based on the resulted value of Sphericity test statistic in eq. (3.30) which compared with a specific threshold value of Λ. From that if the test statistic is less than Λ then the hypothesis H_1 is declared. Hence primary user is present. On the other hand, the null hypothesis H_0 is declared when the Sphericity test statistic is greater than threshold Λ. In this scenario in reality there is a free licensed band. Then the test statistics of both hypotheses written as [11] eq. (3.31).

$$\begin{cases} T_{STD} < \Lambda & \text{for} \quad H_1 \\ T_{STD} > \Lambda & \text{for} \quad H_0 \end{cases} \tag{3.31}$$

3.5.3 John's Detector

John's detector is an optimal for spectrum sensing with small standard deviations of the covariance matrix proportional to the identity matrix. It also a noise-uncertainty free detector with low signal- to- noise ratio. The criterion used to John's detector derived by the Locally Best Invariant Test (LBIT) [44]. Unlike the GLRT criterion, the LBIT criterion often leads to provide a better performance in the low SNR value. The performance of this detector is very good in the presence of multiple primary user detection. Therefore, using the Locally Best Invariant Test (LBIT) can be calculate the test statistics of John's detector which is an importance parameter to decide whether the presence or absence of primary user signal with compared to the specified threshold value Λ. The test statistics of John's detector (T_{SJD}) for multiple primary users can be calculated as [46 eq. (1.2–1.7)];

$$T_{SJD} = \frac{\mathrm{tr}(R^2)}{(\mathrm{tr}(\mathrm{R}))^2} = \frac{\sum_{i=1}^{K} {\lambda_i}^2}{\left(\sum_{i=1}^{K} \lambda_i\right)^2} \tag{3.32}$$

The test statistics from eq. (3.32) compared with the threshold value Λ written as [44].

$$\begin{cases} T_{SJD} > \Lambda & H_1 \\ T_{SJD} < \Lambda & H_0 \end{cases} \tag{3.33}$$

3.6 Interference Based Detection

Interference based detection emphasis to minimize the interference to the primary (licensed) receiver regardless of the licensed transmitter's operation [39]. The signal power received at the licensed receiver reduces exponentially with the distance until it reaches at the level of noise floor. Even if at noise flower point operates the licensed transmitter, but the licensed receiver treats this communication as simply noise and not transmission; hence the unlicensed user can utilize the channel without interfering to the licensed users. That means the cognitive radio users can be transmit its signal with lower transmission power than licensed users to restrict by interference temperature level [32]. Theoretically, there is no licensed user affected by the interference. But, in reality the interference becomes at the receiver. To mitigate this problem the interference temperature classic model is used to measuring the interference temperature as shown in Figure 3.6 announced by the Federal Communication Commission (FCC) [22]. This model indicates the "signal of a radio station designed to operate in the range of received power with the level of the noise floor" [39].

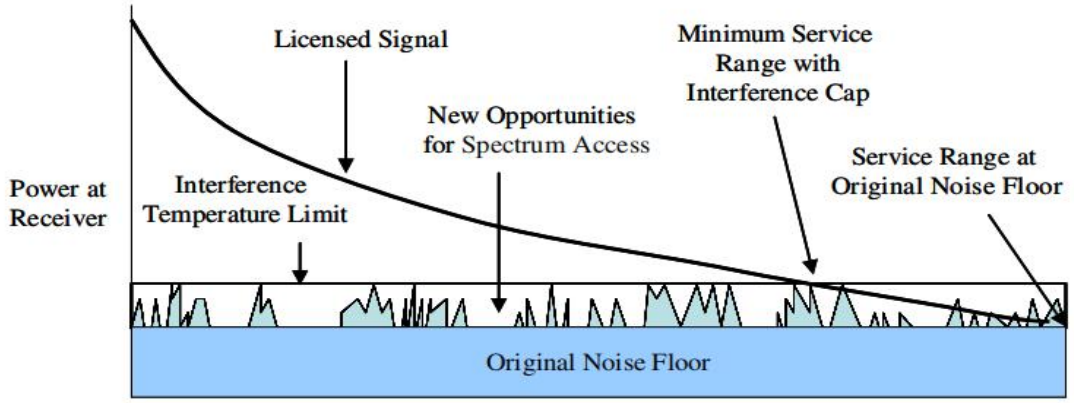

Figure 3.6: "Interference based detection on temperature classic model" [22].

When the noise flower increases at different points within the service area, as indicated by the peaks above the original noise floor then the interfering signals are appeared. The decision of

either or not the presence of a licensed user in the range of frequency band is based on the level of the interference temperature. If the detected licensed signal level is below the interference temperature, the unlicensed user may utilize that channel. Further, if the transmission power of a CR remains below the interference cap, it may utilize any frequency parameters of its choice.

Interference temperature also used to the interpretations of the radio frequency (RF) energy comes from the multiple broadcasts and arrangements with a maximum cap on their collective level. Therefore, for using this spectrum band the SUs couldn't be exceeding the limitation of their transmissions.

3.7 Cooperative Detection

In cooperative spectrum sensing, multiple CR users are collaborated and organized with each other for the exchange of the sensing information and make the final decision to improve the sensing accuracy. Firstly, each CR users are independently performing their sensing by locally (non-cooperatively) scheme and share their sensing information. In this situation each of the cooperating nodes are employs locally using by any sensing methods and sharing the refined sensing information with other nodes based on the selected cooperation strategy [47]. The real method of cooperative spectrum sensing is used to fighting against multipath fading, shadowing and alleviate the tricky of receiver uncertainty as shown in Figure 3.7 [48].

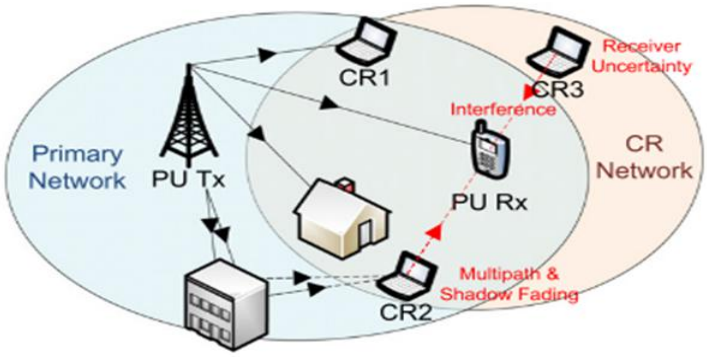

Figure 3.7: Receiver uncertainty and multipath/shadow fading [48].

As shown in the above Figure, "CR1 & CR2 are located inside the transmission range of primary transmitter (PU Tx) while CR3 is outside the range" [48]. CR2 affected by multipath and shadow fading because of the multiple attenuated copies of the PU signal and blocking houses. Therefore, PU's signal may not be correctly detected. In addition to that the broadcast from CR3 may interfere with the reception at PU Rx. This activity happens when the CR3

suffers from the receiver uncertainty problem because of an unawareness of CR3 about PU's broadcast and the presence of the primary receiver (PU Rx).

However, with the help of spatial diversity, the total detection performance can be improved significantly. In a CR network if all spatially distributed CR users can't be simultaneously affected by the fading or receiver uncertainty tricky as shown in the Figure. The greatest observation of a strong primary user signal is by CR1. Hence, using spatial diversity can be minimize the overcome lack of individual interpretations at each CR user by cooperate and share the sensing results with other CR users [48]. Then the decision result is depending on the spatially collected observation of all CR users with combination of their individual decision.

In general context of cooperative spectrum sensing requires some essential components to improve their sensing performance such as PU's, collaborating of CR users with fusion center (FC), the licensed and control channels [48]. Usually, cooperative spectrum sensing involves with control and reporting channels to attain a decision for local sensing. The local sensing is used to create a connection between the CRs and licensed transmitter. The CRs or SUs can report the local sensing data to the FC or share the sensing results with neighbouring nodes by the help of the reporting or common control channel [22]. This process is used to made a decision whether or not the presence of PU in the channel. Based on the collaborating and sensed data sharing the CR user networks categorized as: Centralized, Distributed, and Relay assisted.

3.7.1 Centralized Detection

In a centralized cooperative spectrum sensing scheme, all activities are controlled by the fusion center (FC) or obviously known as the base station (BTS). This type of cooperative sensing performs its detection activities with different levels. Initially, the FC works on the choice of the required frequency band to sensing and prepares all SUs independently perform its local sensing and collaborates. Then all sensing results by cooperating of SUs are reported through the control channel. Finally, the presence or absence of primary user is precise by a FC depending on the received sensing information from cooperative sensing results. On the other, in the case of xG ad-hoc network deployment any SUs work as a FC. Based on the level of its collaboration centralized scheme can be studies as network nodes. Simply the network nodes are cooperating for the purpose of sensing channels. This process knows as a

partially collaborative scheme. In addition to cooperatively sensing of the channel, the nodes can be collaborating to communicate each other known as a collaborative scheme.

3.7.2 Distribution Detection

In this cooperative scheme for making the collaborative decision without requires of the FC rely assisted. Thus, the SUs exchanges the information of local sensing results each other within its transmission range and make a decision individually whether or not the presence of free band (white space) by repetitions. In the distribution spectrum sensing the final decision and the detection results are controlled by the SUs. Therefore, it doesn't involve with any common infrastructure. The decision of the presence or absence of the PUs is made by using the local criterion algorithm. In this algorithm the decision of its presence is based on the satisfaction of the criterion. I.e. if satisfied the criterion then the PU is present if not then SUs send their combined results to other users again and repeat this process until the algorithm is encountered and a decision is gotten. Because of it needs several iterations to reach the decided cooperative decision it takes more time to compare with a centralized detection scheme.

3.7.3 Relay Assisted Detection

Relay-assisted cooperative sensing is a significant for performance improvement gaps of sensing in the control and reporting channel of imperfectness problem. This method is important when some parts of SUs observing weak sensing and strong report channel and the other SUs observing with strong sensing and weak report channel in cooperative spectrum sensing. So, to improve the performance of cooperative spectrum sensing in this scheme both results can be a compliment and collaborate with all results. Relay-assisted cooperative spectrum sensing uses the multi-hop cooperative sensing scheme to forward the sensing result for the intended receiver node [48]. In this scheme, all the intermediate hops are used as relays. Besides this the CR relays are used for forwarding the primary user's traffic.

Chapter 4: Performance Analysis, Test Statistic, Probability of Detection and Threshold

4.1 Introduction

The perfectness of spectrum sensing is decided based on the sensing results such as the quality of factors. In this work concerns on the feature of the performance of the Spherical and John's detector are specified by using the following sensing performance factors are probability of detection (P_D), Probability of false alarm (P_{FA}) and the SNR values.

The probability of detection (P_D) in dynamic spectrum sensing used to the detector makes an accurate decision that channel is employed (the hypothesis H_1). The level of interference security delivered to the licensed or PUs is indicated by the value of P_D. That means the large value of P_D indicates the correct sensing with the small effect of interference. In this work, can be observe the detection probability versus SNR, detection probability at the different false alarm probability, and interpretations of the receiver operating characteristics curves. The false alarm existence happens when the detector interprets H_1(primary signal is present), but H_0 is the correct decision (primary signal is absent). This occurrence of probability is considered as the false alarm probability. When there is a false alarm then the unlicensed users or secondary users couldn't exploit the spectrum hole. In this condition, there is a loss of free channel usage opportunity. In order to get the more efficient performance in spectrum sensing parameters should be kept P_{FA} is low and $P_D$is high [10].

Some significant matters are measured in this study such as exploiting the dynamic spectrum sensing correctness, minimizing the interference to the PUs by maximizing the probability of detection and to increases the SUs throughputs by minimizing the false alarm probability P_{FA}.

4.2 Performance Measurement

The receiver performance is quantified by showing curves of the probability of detection against SNR values ($P_D$versus SNR) and the receiver operating characteristics (ROC) curves. These curves serve as a tool to select and study the performance of a sensing scheme. The detection probability versus signal-to-noise ratio graph illustrations are shows the relationships between detection probability and signal-to-noise ratio that used to determine the best scheme. The complementary receiver operating characteristics (ROC) curves show the probability of detection (P_D) versus probability of false alarm (P_{FA}). These curves enable

exploration of the relationship between sensitivity (probability of detection) and specificity (false alarm rate) [49]. To study the different situations of interest by plot the ROC curves with varying one parameter and the other parameters are fixed.

4.3 Probability of Detection and Test Statistic for Spherical Detector

By considered the vector form of the received signal expressed as [31] in eq. (4.1);

$$x = \text{Hs} + \eta \tag{4.1}$$

Where, $x \in C^{kp\times N}$ is a dimensional complex vector, which represents the receiving data vector to sense P primary users.

The K×1 vector η denotes the additive complex Gaussian noise vector with independent and identical distributed (i.i.d) N ~ $(0, \partial_\eta^2 I_K)$ having zero mean and covariance matrix $\partial_\eta^2 I_K$. The K×P dimensional matrix H = $[h_1, h_2, \ldots, h_P]$ denotes coefficients of the channel gain.

Without assumption of channel model H specification in the absence of PUs sample covariance matrix R=XX^H follows an uncorrelated non-central complex Wishart distribution R ~ W_K (N, Σ) with population covariance matrix Σ. Then the corresponding Σ calculated for hypothesis H_0 as follows [44] eq. (4.2);

$$\Sigma = \text{E}[R]/\text{N} = \partial_\eta^2 I_K \tag{4.2}$$

Where ∂_η^2 is the noise power, I_K is $K \times K$ identity matrix and X is calculated from in eq. (3.23). Hence the received signals are containing only noise vectors. On the other hand, under the presence of PU signal sample (hypothesise H_1) R follows a correlated non-central complex Wishart distribution R ~ W_K (N, Σ) of the population covariance matrix Σ can be calculated as [44] in eq. (4.3);

$$\Sigma = \partial_\eta^2 I_K + \sum_{p=1}^{P} \vartheta_p h_p h_p^H \tag{4.3}$$

Where $\vartheta_p = E[s_p s_p^H]$ is the transmitted power of the P$^{\text{th}}$ primary user signal and s_p^H is the Hermitian complex conjugate sample values of primary transmitted signals. In this scenario the analysis included in the presence of primary user signal and noise signal vectors. Then the received signal to noise ratio (SNRγ) of primary user P can be calculated as [11];

$$\gamma = \frac{\vartheta_p \|h_p\|^2}{\partial_\eta^2} \tag{4.4}$$

4.3 Test Statistics and Probability of Detection for Spherical Detector

The test statistics of Spherical detector (T_{STD}) is an important term and the 1st essential consideration from SUs perspective in order to get the awareness of the presence or absence of active PUs. From eq. (4.3) perspective the fact that $\sum_{p=1}^{P} \vartheta_p h_p h_p^H$ is a positive definite matrix. By repeating eq. (4.2) and taking the difference between eq. (4.3) and (4.2) for hypothesis test in the multiple PUs scenario [11] written as in eq. (4.5) & (4.6) respectively;

$$\Sigma = \partial_\eta^2 I_K \qquad H_0 \tag{4.5}$$

$$\Sigma > \partial_\eta^2 I_K \qquad H_1 \tag{4.6}$$

In this case except positive definite matrix which is defined as with the assumption of Z>Y represents Z−Y all are assumed to be blind (not required prior knowledge of the primary transmitted signal), i.e. ∂_η^2 , Σ and number of PUs are blind [11].

The test statistics of Spherical based (T_{STD}) detector was written under the general likelihood ratio test (GLRT) criterion [43] and it can be separate from a constant, by using the likelihood function of the data matrix X written as;

$$L(X/\Sigma) = (|\Sigma|)^{-N} e^{tr(\frac{-R}{\Sigma})} \tag{4.7}$$

Where, $|\Sigma|$ the determinant of population covariance matrix and X is calculated from in eq. (3.23). Then the likelihood ratio statistics represented by ρ written as [11];

$$\rho = \frac{sup_{\partial_\eta^2 > 0} \mathrm{L}(\mathrm{X}/\partial_\eta^2 I_K)}{sup_{\Sigma > 0} \mathrm{L}(\mathrm{X}/\Sigma)} \tag{4.8}$$

The maximum likelihood (ML) estimates of ∂_η^2 for H_0 and Σ for H_1 are expressed [45] respectively;

$$\widehat{\partial_\eta^2} = \frac{tr(R)}{KN} \tag{4.9}$$

$$\widehat{\Sigma} = \frac{R}{N} \tag{4.10}$$

By substituting eq. (4.9) and (4.10) to eq. (4.8) [11];

$$\rho^{1/N} = \frac{|\mathrm{R}|}{(\frac{1}{K}\mathrm{tr}(\mathrm{R}))^K} = T_{STD} \tag{4.11}$$

Where $tr(R)$ is the trace of observed sample covariance matrix R.

From eq. (4.11) the hypothesis H_0 is rejected when $\rho^{1/N}$ is small. Hence from the test statistics T_{STD} can be made the decision H_0 *and* H_1 at specified threshold Λ written as [11] eq. (4.12) and (4.13) respectively;

$$\begin{cases} T_{STD} > \Lambda & H_0 \quad (4.12) \\ T_{STD} < \Lambda & H_1 \quad (4.13) \end{cases}$$

The sample covariance matrix R follows uncorrelated complex Wishart distribution to offers for approximation depart the hypothesis H_0. While a correlated complex Wishart distribution for H_1. Then the random variable distribution of T_{STD} deals as approximative moments which sample covariance matrix R follows uncorrelated complex Wishart distribution W_K (N, I_K) for H_0 and correlated complex Wishart distribution $W_K(\mathrm{N}, \Sigma)$ for H_1 [11] with probability density function in eq.(4.14);

$$R \sim \begin{cases} \frac{1}{\mathbb{\Gamma}_K(N)} (|\mathrm{R}|)^{N-K} e^{tr(-R)} & H_0 \\ \frac{1}{\mathbb{\Gamma}_K(N)(|\Sigma|)^N} (|\mathrm{R}|)^{N-K} e^{tr(-\Sigma^{-1}\mathrm{R})} & H_1 \end{cases} \quad (4.14)$$

Where Γ $(\cdot)$ is the gamma function. From the T_{STD} identify H_1 correctly or H_0 incorrectly defines as the detection probability P_D, and false alarm probability P_{FA} [32] in eq. (4.15) & (4.16) respectively;

$$P_D = P(T_{STD} < \Lambda / H_1) \quad (4.15)$$

$$P_{FA} = P(T_{STD} > \Lambda / H_0) \quad (4.16)$$

The P_{FA} and P_D can be calculated in terms of cumulative density function (CDF) with decision threshold Λ [11]; therefore, by using eq. (4.12) and (4.13) for any threshold Λ of the P_{FA} and P_D can be calculated by using the following Proposition 1 & 2.

Proposition 1: The CDF is represented by F_{STD} with any sensor size K and sample size N can be analysis using the two-first-moment Beta approximation to the CDF of T_{STD} for H_0 [11] as follows;

$$F_{STD}(y) \approx \frac{\beta_y(\alpha_0, \beta_0)}{\beta(\alpha_0, \beta_0)}, \quad y \in [0,1] \quad (4.17)$$

Where $\beta_y(\alpha_0, \beta_0) = \beta_y(\alpha_0, \beta_0) = (1-y)^{\beta_0} \sum_{j=\alpha_0}^{\infty} \binom{\beta_0+j-1}{j} y^j$ represent the incomplete beta function and $\beta(\alpha_0, \beta_0) = \frac{\mathbb{\Gamma}((\alpha_0)\mathbb{\Gamma}(\beta_0)}{\mathbb{\Gamma}(\alpha_0+\beta_0)} \sim \sqrt{2\pi} \frac{\alpha_0^{\alpha_0-1/2} \beta_0^{\beta_0-1/2}}{(\alpha_0+\beta_0)^{\alpha_0+\beta_0-1/2}}$ is the beta function. The

completed proof is in Appendix A. The factors α_0 and β_0 are simple functions of the sensor size K and sample size N which are given by [11];

$$\alpha_0 = \frac{M_1(M_1-M_2)}{M_2-(M_1)^2}, \qquad \beta_0 = \frac{(1-M_1)(M_1-M_2)}{M_2-(M_1)^2} \tag{4.18}$$

By using the asymptotic T_{STD} distributions of the complex Wishart matrices and using T_{STD} in eq. (4.12), for any threshold Λ of the false alarm probability is calculated as $P_{FA}(\Lambda)$ [50];

$$P_{FA}(\Lambda) = F_{STD}(\Lambda) = \frac{\beta_{\Lambda}(\alpha_0, \beta_0)}{\beta(\alpha_0, \beta_0)} \tag{4.19}$$

Equivalently for any P_{FA} a threshold can be written by numerically inverting the $F_{STD}(\Lambda)$;

$$\Lambda = F_{STD}^{-1}(P_{FA}) \tag{4.20}$$

From the threshold Λ (4.20) can be obtain the probability of false alarm P_{FA} in eq. (4.21).

$$P_{FA} = F_{STD}(\Lambda) \tag{4.21}$$

Typically, P_{FA} is between $[10^{-1}, 10^{-2}]$ which is the IEEE 802.22 standard recommends P_{FA} <0.1 for spectrum sensing [51].

Proposition 2: On the other hand, to calculate the P_D for any sensor size K and sample size N, by analysis the two-first-moment Beta-approximation to the CDF of T_{STD} for H_1 is [11];

$$F_{STD\,P_D}(y) \approx \frac{\beta_y(\alpha_1, \beta_1)}{\beta(\alpha_1, \beta_1)}, \qquad y \in [0,\infty) \tag{4.22}$$

Where $\alpha_1 \, and \, \beta_1$ are calculated as;

$$\alpha_1 = \frac{N_1(N_1-N_2)}{N_2-(N_1)^2}, \qquad \beta_1 = \frac{(1-N_1)(N_1-N_2)}{N_2-(N_1)^2} \tag{4.23}$$

$$N_n \approx (K)^{\mathrm{Kn}}\left(\frac{\mathbb{\Gamma}\left(\alpha_1 - \mathrm{Kn}\right)\mathbb{\Gamma}_{\mathrm{K}}(\mathrm{N}+\mathrm{n})(|\Sigma|)^{\mathrm{n}}}{\mathbb{\Gamma}_{\mathrm{K}}(\mathrm{N})\mathbb{\Gamma}(\alpha_1)}\right. \tag{4.24}$$

Where N_n are the n[th] moments of beta and N is the number of samples. The completed proof is in Appendix B. By using T_{STD} eq. (4.13), for any threshold Λ the detection probability is calculated as $P_D(\Lambda)$;

$$P_D(\Lambda) = F_{STD\,P_D}(\Lambda) = \frac{\beta_\Lambda(\alpha_1,\ \beta_1)}{\beta(\alpha_1,\ \beta_1)}, \tag{4.25}$$

For quite affordable of computational complexity of threshold calculation is needed additional approximate of the parameters (α_0, β_0) and (α_1, β_1) to their particular nearest of non-negative integer. Therefore, both eq. (4.19) & (4.25) reduce to simple polynomial equations of Λ. For a target of the P_{FA} to calculate the resulting threshold Λ from eq. (4.20) and this threshold is equivalent to the P_D can be found from eq. (4.25). From this the relation between P_{FA} & P_D is known as complementary receiver operating characteristics curve (ROC) can be obtained as:

$$P_D = F_{STD\,P_D}(F_{STD}^{-1}(P_{FA}) \tag{4.26}$$

The above is the P_D on AWGN channel but with Rayleigh multipath fading channel, which is more commonly experienced in realistic wireless networks [31]. In Rayleigh fading channels, the instantaneous SNR has the following probability distribution function (PDF) [52] eq. (4.27);

$$f_{R\gamma}(\gamma) = \frac{1}{\overline{\gamma}} e^{\frac{\gamma}{\overline{\gamma}}}, \qquad \gamma \geq 0 \tag{4.27}$$

Where "γ and $\overline{\gamma}$ represent the instantaneous and the average SNR respectively" [52]. To considered only P_D, the detection probability in averaging, since it is a function of SNR as shown in eq. (4.25). Thus, the average P_D of the Rayleigh fading channel [31] calculated as;

$$\overline{P}_{DRay} = \int_0^\infty (\Lambda,\ \gamma)\ f_{R\gamma}(\gamma)\, d\gamma \tag{4.28}$$

By substituting eq. (4.25) and (4.27) in to (4.28);

$$\overline{P}_{DRay} = \int_0^\infty \frac{\beta_\Lambda(\alpha_1,\ \beta_1)}{\beta(\alpha_1,\ \beta_1)}\ \frac{1}{\overline{\gamma}} e^{\frac{\gamma}{\overline{\gamma}}}\ d\gamma \tag{4.29}$$

By substitute the value of the in complete beta function

$\beta_\Lambda(\alpha_1,\ \beta_1) = (1-\Lambda)^{\beta_1} \sum_{j=\alpha_1}^{\infty} \binom{\beta_1+j-1}{j} \Lambda^j$ and beta function $\beta(\alpha_1,\ \beta_1) = \frac{\mathbb{\Gamma}(\alpha)\mathbb{\Gamma}(\beta)}{\mathbb{\Gamma}(\alpha+\beta)} \sim \sqrt{2\pi}\frac{{\alpha_1}^{\alpha_1-1/2}{\beta_1}^{\beta_1-1/2}}{(\alpha_1+\beta_1)^{\alpha_1+\beta_1-1/2}}$;

$$\overline{P}_{DRay} \approx \int_0^{\infty} \frac{(1-\Lambda)^{\beta_1} \sum_{j=\alpha_1}^{\infty} \binom{\beta_1+j-1}{j} \Lambda^j}{\sqrt{2\pi}\frac{\alpha_1{}^{\alpha_1-1/2}\beta_1{}^{\beta_1-1/2}}{(\alpha_{1+}\beta_1)^{\alpha_1+\beta_1-1/2}}} \frac{1}{\overline{\gamma}} e^{\frac{\gamma}{\overline{\gamma}}}\, d\gamma \tag{4.30}$$

Similarly, for John's detector the average probability of detection P_D under Rayleigh fading channel calculated as;

$$\overline{P}_{DRay} = \int_0^{\infty} \frac{\beta_{\Lambda}(\frac{K(1-\Lambda)}{K-1};\ \alpha_1,\ \beta_1)}{\beta(\alpha_1,\ \beta_1)} \frac{1}{\overline{\gamma}} e^{\frac{\gamma}{\overline{\gamma}}}\, d\gamma \tag{4.31}$$

Where $\beta_{\Lambda}(\frac{K(1-\Lambda)}{K-1};\ \alpha_1,\ \beta_1) = \int_0^{\frac{K(1-\Lambda)}{K-1}} \frac{K(1-\Lambda)}{K-1}^{\alpha_1-1} (1-\frac{K(1-\Lambda)}{K-1})^{\beta_1-1} d\Lambda$ is the incomplete beta function and $\beta(\alpha_1,\ \beta_1) = \frac{\mathbb{\Gamma}(\alpha)\mathbb{\Gamma}(\beta)}{\mathbb{\Gamma}(\alpha+\beta)} \sim \sqrt{2\pi}\frac{\alpha_1{}^{\alpha_1-1/2}\beta_1{}^{\beta_1-1/2}}{(\alpha_{1+}\beta_1)^{\alpha_1+\beta_1-1/2}}$ is the beta function. So, by substitution this functions in to eq. (4.30).

$$\overline{P}_{DRay} \approx \int_0^{\infty} \frac{\int_0^{\frac{K(1-\Lambda)}{K-1}} \frac{K(1-\Lambda)}{K-1}^{\alpha_1-1} (1-\frac{K(1-\Lambda)}{K-1})^{\beta_1-1} d\Lambda}{\sqrt{2\pi}\frac{\alpha_1{}^{\alpha_1-1/2}\beta_1{}^{\beta_1-1/2}}{(\alpha_{1+}\beta_1)^{\alpha_1+\beta_1-1/2}}} \frac{1}{\overline{\gamma}} e^{\frac{\gamma}{\overline{\gamma}}}\, d\gamma \tag{4.32}$$

Where, $P_D(\Lambda) \approx \frac{\beta_{\Lambda}(\frac{K(1-\Lambda)}{K-1};\ \alpha_1,\ \beta_1)}{\beta(\alpha_1,\ \beta_1)}$ is calculated in the next section with detailed description and present in eq. (4.55).

4.4 Test Statistics and Probability of Detection for John's Detector

In the assumption of spectrum sensing situation, for P ≥ 1 PUs transmitting within the frequency band of interest has the central frequency f_c and the bandwidth W with transmission sample duration of T ≤ 1/W. Also, assumed with the minimum bandwidth transmissions of primaries within W, matching to the sample duration T_{smax}.

There is a detector with K sensors trying to detect the presence of PUs. Again, assumed there are multipath channels between the PU and the detector. The number of PUs, and the multipath structure of these users, is blind to the detector. But all possible sample durations between T and T_{smax} of PUs are known to the detector. Then the received signal x(t) after filtering in complex baseband signal at K sensors in the bandwidth of interest is [44];

$$x(\mathrm{t}) = \sum_m \sum_{p=1}^{P} s_{p,m} h_p \left(t - mT_p + d_p\right) + \eta(\mathrm{t}) \tag{4.33}$$

Where $T_p = s_p T$ is the sample duration for transmitter p, h_p(t) is the convolution of the reception filter with transmission filter of p, and the vector of channel impulse responses between p and K sensors. The sum over m is the train of transmission samples, and the variable d_p is the differences in symbol timing and transmitter propagation delay. Let the K-sensor detector chooses s_s to be the least common possible values of $s_{p,}$ and takes samples every s_sT second gives [44];

$$x = \sum_m \sum_{p=1}^{P} s_{p,\,m} h_p \left(n s_s - m s_p\right) T + d_p) + \eta \tag{4.34}$$

Representing $h_{p,m} = h_p\big((m s_p)T + d_p\big)$ then eq. (4.34) becomes;

$$x = \sum_{p=1}^{P} \sum_{m=1}^{M} s_{p,nr_p - m}\, h_{p,m} + \eta \tag{4.35}$$

Where $r_p = s_s/s_p$ is the independent transmission samples transmitted by primary per received sample taken. By assumed causality the earliest time of a sample affects the received signal, as well as a maximum delay spread M [44]. Note that the number of multipath components depends importantly on the pulse shapes used by the transmitters, the receiver filter, and whether the detector is synchronized to one or more of the transmitters [44].

For the received signal detection by considering the two hypotheses: Null hypothesis (H_0) or the received signal contains only noise vector at the cognitive radio network (CRN) and hypothesis H_1or the received signal vector have with signal plus noise vector. Then the two hypotheses can be written as an assembling, the MP transmitted samples s_p, nr_p-m in to vector form [44] written as in eq. (4.36 & 4.37).

$$x = \eta \tag{4.36}$$

$$x = \mathrm{Hs} + \eta \tag{4.37}$$

Where, $x \in C^k$ is the received data vector and K×PM dimension matrix, H= $[h_{1,1}, h_{1,2}, ..., h_{1,M}, h_{2,1}, ..., h_{P,M}]$ denotes the M-tap channels between P primary users and K sensors. By assumption of proper filtering K×1 vector η denotes the additive complex Gaussian noise vector with zero mean and covariance matrix $\partial_\eta^2 I_K$. By collect N observations from eq. (4.37) to a K$\times N$ received data matrix X= $[x_1, x_2, ...x_N] = HS$. Where the signal vectors $S = [s_1, s_2, ...s_N]$. Based on the data matrix X can be decide the presence or absence of PUs by calculated as the sample covariance matrix R=XX^H which follows uncorrelated and correlated non-central complex Wishart distribution R ~ W_K (N, Σ) with population

covariance matrix Σ. Then the corresponding Σ calculated under hypothesis H_0 and H_1written as [44] in eq. (4.38) & (4.39) respectively;

$$\Sigma = \mathrm{E}\,[R]/\mathrm{N} = \partial_\eta^2 I_K \tag{4.38}$$

$$\Sigma = \partial_\eta^2 I_K + \sum_{p=1}^{P} \vartheta_p h_p h_p^H \tag{4.39}$$

Using the sample covariance matrix R can be calculate the test statistics of John's detector (T_{SJD}) [53, (1.2-1.7)] in eq. (4.40);

$$T_{SJD} \cong \frac{tr(R^2)}{(tr(R))^2} = \frac{\sum_{i=1}^{K} {\lambda_i}^2}{(\sum_{i=1}^{K} \lambda_i)^2}, \qquad [1/\mathrm{K},\ 1] \tag{4.40}$$

Where, λ_i is the order eigenvalues of sample covariance matrix R [53]. The T_{SJD} is a significant parameter to make the decision whether or not the presence of PUs made the comparison with a specified threshold Λ [44] in eq. (4.41).

$$\begin{cases} T_{SJD} < \Lambda & H_0 \\ T_{SJD} > \Lambda & H_1 \end{cases} \tag{4.41}$$

With natural support [1/K, 1] of T_{SJD}. Then with starting of the m^{th} moments analyse to T_{SJD} for H_0 [44];

$$E\left[{T_{SJD}}^m\right] = \frac{E[(\sum_{i=1}^{k} {\lambda_i}^2)^m]}{E\left[\left(\sum_{i=1}^{k} \lambda_i\right)^{2m}\right]} \tag{4.42}$$

The derivation of m^{th} moments of non-negative integer for complex Wishart matrix distribution expressed in proposition 3 [44]:

Proposition 3: The m-th non-negative integer moment of random variable to T_{SJD} for H_0 is [45];

$$M_m = \frac{C\,\mathbb{\Gamma}(KN)}{\mathbb{\Gamma}(2m+KN)} \sum_{a_1+\ldots+a_K=m} \frac{m!}{a_1!\ldots a_K!} \times \prod_{1\le i<j\le K} (2a_j - 2a_i + j - i) \prod_{i=1}^{K} \mathbb{\Gamma}(2a_i + N - K + i) \tag{4.43}$$

Here $a_1 + \ldots + a_K = m$ is the sum of overall non-negative integer and,
C = $(\prod_{i=1}^{K} \mathbb{\Gamma}(N-i+1)\mathbb{\Gamma}(K-i+1))^{-1}$ is a constant.

For exact distribution of T_{SJD} easily construct an approximative T_{SJD} distribution by matching its moments to some known distribution with the same support [44]. It is often the case that for the same statistics, the functional form of its distributions in both real and complex Wishart cases remains the same [54]. For the real Wishart under H_0, the exact T_{SJD} distributions for K=2, 3 hold the same polynomial form as the Beta distribution [55]. Furthermore, the Beta distribution was shown to correctly model the distribution of T_{SJD} for random K [56]. From these evidences, by selection of Beta distribution approximate to T_{SJD} for complex Wishart distribution expressed in proposition 4:

Proposition 4: For any sensor size K and sample size N, the Beta approximation of the CDF to T_{SJD} for H_0 and using eq. (4.43) the exact two first moments [44] written in eq. (4.44);

$$F_{SJD}(\mathrm{y}) \approx 1 - \frac{\beta_{\mathrm{y}}(\frac{K(1-y)}{K-1};\ \alpha_0,\ \beta_0)}{\beta(\alpha_0,\ \beta_0)}, \qquad \mathrm{y} \in [\frac{1}{k}, 1] \tag{4.44}$$

Where $\beta_{\mathrm{y}}(\frac{K(1-\mathrm{y})}{K-1}; \alpha_0, \beta_0) = \int_0^{\frac{K(1-\mathrm{y})}{K-1}} \frac{K(1-\mathrm{y})}{K-1}^{\alpha_0-1} (1 - \frac{K(1-\mathrm{y})}{K-1})^{\beta_0-1} d\mathrm{y}$ is describes as incomplete lower beta function and, α_0 and β_0 are calculated as;

$$\alpha_0 = \frac{(KM_1-1)(KM_1-KM_2+M_1-1)}{(K-1)K(M_2-{M_1}^2)}, \qquad \beta_0 = \frac{(M_1-1)(KM_1-KM_2+M_1-1)}{(K-1)({M_1}^2-M_2)} \tag{4.45}$$

Where M_1 and M_2 are the 1st and the 2nd moments of T_{SJD}.

From the T_{SJD} (4.41) and Proposition 4, the resulting approximation to the probability of false alarm for a given threshold Λ [44] is given as in eq. (4.46);

$$P_{FA}(\Lambda) = 1 - F_{SJD}(\Lambda) \approx \frac{\beta_{\Lambda}(\frac{K(1-\Lambda)}{K-1};\ \alpha_0,\ \beta_0)}{\beta(\alpha_0,\ \beta_0)} \tag{4.46}$$

Where, $\Lambda \in [1/K, 1]$. From this for any P_{FA} requirement a threshold can be derived numerically by inverting $P_{FA}(\Lambda)$ [44] (4.47);

$$\Lambda = {F_{SJD}}^{-1}(1 - P_{FA}) \tag{4.47}$$

4.5 Probability of Detection

For suitability by considering and define the random variables x, y & z to studies the moments of T_{SJD} for H_1 [44] in eq. (4.48).

$$x = \frac{1}{N^2} tr(R^2), \quad y = \frac{1}{N} tr(R), \quad z = \frac{x}{y^2}. \tag{4.48}$$

Obviously, z is the random variable which gives attention to T_{SJD}. Unlike the case of H_0, the equality (4.42) no longer holds under H_1[45]. In order to estimate the moments of z it is not enough to estimate the moments of random variables x and y separately, estimating their correlation is needed [44]. Simple and accurate estimates of the mean and variance of z for H_1, which involve the first two exact moments and the covariance of random variables x and y [44].

$$\mu_x = tr(\Sigma^2) + \frac{1}{N}(\mathrm{tr}(\Sigma))^2 \tag{4.49}$$

$$\mu_{xy} = \frac{2}{N} tr(\Sigma^3) + \frac{2}{N^2} \mathrm{tr}(\Sigma)\mathrm{tr}(\Sigma^2) \tag{4.50}$$

$$\mu_z \approx \frac{\mu_x}{{\mu_y}^2} - \frac{2\mu_{xy}}{{\mu_y}^3} + \frac{3\mu_x v_y}{{\mu_y}^4} \tag{4.51}$$

$$v_z = \frac{v_x}{{\mu_y}^4} - \frac{4\mu_x \mu_{xy}}{{\mu_y}^5} + \frac{4{\mu_x}^2 v_y}{{\mu_y}^6} \tag{4.52}$$

Hence μ_{xy} is the covariance of x and y.

$$v_x = \frac{4}{N} tr(\Sigma^4) + \frac{2}{N^2}(4\mathrm{tr}(\Sigma)\mathrm{tr}(\Sigma^3) + (\mathrm{tr}(\Sigma^2))^2) + \frac{2}{N^3}(2(\mathrm{tr}(\Sigma))^2 \mathrm{tr}(\Sigma^2) + tr(\Sigma^4)) \tag{4.53}$$

$$\mu_y = tr(\Sigma) \tag{4.54}$$

$$v_y = \frac{1}{N} tr(\Sigma^2) \tag{4.55}$$

With the estimates of the mean (4.51) and variance (4.52), closed-form distributions of T_{SJD} for H_1 can be constructed [44]. Also select the Beta distribution in Appendix C eq. (4.89), thus it has the same support as T_{SJD}. Accordingly, I have distribution under H_1 holds the same form as the Proposition 5:

Proposition 5: For any sensor size K and sample size N, the Beta approximation to the CDF of T_{SJD} for H_1 derived on the estimated value of the two first moments in eq. (4.51) and (4.52), is equals [51];

$$F_{SJDP_D}(\mathrm{y}) \approx 1 - \frac{\beta_\Lambda(\frac{K(1-y)}{K-1};\ \alpha_1,\ \beta_1)}{\beta(\alpha_1,\ \beta_1)}, \qquad \mathrm{y} \in [\frac{1}{k}, 1] \tag{4.56}$$

Where α_1 and β_1 are calculated as:

$$\alpha_1 = \frac{(1-K\mu_z)(\mu_z-1)(K\mu_z-1)+Kv_z}{(K-1)K\mu_z}, \qquad \beta_1 = \frac{(\mu_z-1)(\mu_z-1)(K\mu_z-1)+Kv_z}{(K-1)\mu_z} \tag{4.57}$$

From the T_{SJD} for H_1 (4.41) and Proposition 5, the probability of detection approximation is.

$$P_D(\Lambda) = 1 - F_{SJDP_D}(\Lambda) \approx \frac{\beta_\Lambda(\frac{K(1-\Lambda)}{K-1}; \alpha_1, \beta_1)}{\beta(\alpha_1, \beta_1)} \tag{4.58}$$

The closed-form of approximative false alarm probability using eq. (4.56) and the detection probability from eq. (4.58), the analytical ROC expression for John's detector is obtained as:

$$P_D = 1 - F_{SJDP_D}({F_{SJD}}^{-1}(1 - P_{FA}) \tag{4.59}$$

The parameters a_0, β_0 in eq. (4.55) and a_1, β_1 in eq. (4.57) are only the elementary functions of the sensor size K, the sample size N and the population covariance matrix Σ. Therefore, P_D is depending on these parameters.

4.6 Cooperative Spectrum Sensing Over Rayleigh Fading Channel

The signal detection performance of cognitive users would be depreciated due to wireless communication system environments such as shadowing, deep fading, and hidden node terminal problems. To solve this problem the spectrum sensing is achieved by many cognitive radios cooperatively. Whereas cooperative gain such as improved detection performance and relaxed sensitivity requirement can be achieved [48]. Cooperative sensing can suffer to any additional sensing time, delay, energy, and operations devoted to its sensing and any performance degradation affected by it [48]. Recently works show that cooperative spectrum sensing to provide a better detection capability and at the same time reduce the false alarm probability over Rayleigh fading channel [57]. Consider N CR users share the sensing data cooperatively to improve the detection performance. It is assumed that every CR user has the same fading and noise statistics in the S-channel. More exactly, an independent and identically distributed statistics are assumed in the S-channels of the CR users present in the network. By consider that the channels between CRs and FC are ideal. Using soft-data fusion operations which decision is based "on the energy values obtained from the different cognitive radio (CR) users are achieved at fusion center (FC) and the final decision on the status of a primary user (PU) is made" [59]. Therefore, the signals from multiple CR users are combined to achieve the improved average SNR. There are different types of soft-data fusion schemes. But in this thesis work, consider only the selection combining (SC) scheme which

is a best significant to increases the spectral efficiency in cooperative spectrum sensing. The selection combiner output of the signal-to-noise ratio expressed as [58];

$$\gamma_{sc} = \max\ (\gamma^1,\ \gamma^2, \ldots..,\gamma^N) \tag{4.60}$$

The probability of detection in soft data fusion scheme is expressed in terms of SNR γ of the S-channel SNR under any fading scenario, by averaging P_D of any fusion scheme, the average overall detection probability $\overline{P}_D$ given as [59];

$$\overline{P}_D = \int_0^{\infty} P_D\, f_{R\gamma}(\gamma)\, d\gamma \tag{4.61}$$

Selection Combining fusion in Rayleigh fading: For Rayleigh fading channel by assuming S-channels with average SNR of $\overline{\gamma}$ per-channel inserting the PDF and CDF [60] of the expression for combiner output SNR PDF is written as [58];

$$f_{R\gamma_{sc}}(\gamma_{sc}) = \frac{N}{\overline{\gamma}}[1 - \exp\,(-\frac{\gamma_{sc}}{\gamma_{sc}})]^{N-1} \times\ \exp\,(-\frac{\gamma_{sc}}{\gamma_{sc}})\,, \quad \gamma_{sc} \geq 0 \tag{4.62}$$

Using the relation [61 (4.13)];

$$[1 - \exp\,(-x)]^N = \sum_{k=0}^{N} \binom{N}{k} (-1)^k exp(-kx) \tag{4.63}$$

In appropriate form of the $f_{R\gamma_{sc}}(\gamma_{sc})$ in (4.62) re-written as;

$$f_{R\gamma_{sc}}(\gamma_{sc}) = N \sum_{k=0}^{N-1} \frac{(-1)^k}{k+1} \binom{N-1}{k} \frac{1}{\overline{\gamma}/_{(k+1)}} \times exp(\frac{\gamma_{sc}}{\overline{\gamma}/_{(k+1)}})\,, \qquad \gamma_{sc} \geq 0 \tag{4.64}$$

From eq.(4.64) can be calculate the probability of detection for the Spherical & John's detector under selection combining scheme with Rayleigh fading channel written as in eq.(4.65) & (4.66) respectively: By replacing the value of $f_{R\gamma_{sc}}(\gamma_{sc})$ from eq. (4.64) instead of $\frac{1}{\overline{\gamma}} e^{\frac{\gamma}{\overline{\gamma}}}$ to (4.61) can gives eq. (4.65).

$$\overline{P}_{D,\,sc,Ray} \approx N \sum_{k=0}^{N-1} \frac{(-1)^k}{k+1} \binom{N-1}{k} \frac{k+1}{\overline{\gamma}} \times \int_0^{\infty} \frac{(1-\Lambda)^{\beta_1} \sum_{j=\alpha_1}^{\infty} \binom{\beta_1+j-1}{j} \Lambda^j}{\sqrt{2\pi} \frac{\alpha_1^{\alpha_1-1/2} \beta_1^{\beta_1-1/2}}{(\alpha_1+\beta_1)^{\alpha_1+\beta_1-1/2}}} \exp\,(\frac{(k+1)\gamma_{sc}}{\overline{\gamma}})\, d\gamma_{sc} \tag{4.65}$$

$$\overline{P}_{D,\,sc,Ray} \approx N \sum_{k=0}^{N-1} \frac{(-1)^k}{k+1} \binom{N-1}{k} \frac{k+1}{\overline{\gamma}} \times \int_0^{\infty} \frac{\int_0^{\frac{K(1-\Lambda)}{K-1}} \frac{K(1-\Lambda)}{K-1}^{\alpha_1-1} (1-\frac{K(1-\Lambda)}{K-1})^{\beta_1-1} d\Lambda}{\sqrt{2\pi} \frac{\alpha_1^{\alpha_1-1/2} \beta_1^{\beta_1-1/2}}{(\alpha_1+\beta_1)^{\alpha_1+\beta_1-1/2}}} \exp\,(\frac{(k+1)\gamma_{sc}}{\overline{\gamma}})\, d\gamma_{sc} \tag{4.66}$$

Chapter 5: Simulation Results and Discussions

In the previous Chapters describe about the ideas and theoretical background of Spherical and John's detection methods is presented. In this chapter, the simulation results by using Matlab2013a based on the methods and interpretation of the results is included. The performance comparison limitations are analysed based on detection probability versus SNR, false alarm probability, and by balancing receiver operating characteristics curve (ROC) over Rayleigh fading channel scenario for P≥ 1 primary users and more than two secondary users which detect the primary signal cooperatively to check presence or absence of primary users. In addition to that the simulations are achieved by Monte Carlo method which uses for random signals in stochastic methods. The simulation parameters which uses for this work are listed below in Table 5.1.

Table 5.1: Simulation parameters

Simulation of Parameters	Values or Types
Number of transmitter and receiver	≥2
Number of PUs	≥1
Number of SUs	[4, 6]
Transmission bandwidth	7Mhz
Center frequency	5MHz and 6MHz
Modulation	BPSK
Noise	White Gaussian
Channel	Rayleigh Fading channel
Number of samples	10,000
Number of Monte Carlo	100,000
SNR interval	[-20,0] dB
Cooperative network	Soft fusion-center with SC scheme
Detection Probability	1
False alarm Probability	≤0.1
Detector	Spherical and Johnson's

5.1 Comparison of Detection Performance on Different SNR Values

Figure 5.1 shows the relationship between the detection probability and the SNR for the case of a single licensed user (PU) detected by four cognitive radio users (SUs) in cooperative

scheme. The results show that for a low SNR values between range of [-20, 0] dB and 0.1 probability of false alarm. As illustrated in Figure 5.1 the results of Spherical detector using GLRT or MLRT estimator gives the good detection performance which compared to John's using LBIT estimator. On the other hand, both of the Spherical and John's detection probability shows the increments with SNR. Also, in observing the final result of both detectors gives unity probability of detection performance at SNR values of 0dB. That means at the value of less than 0dB SNR both of Spherical and John's detection methods are affected by interference for the PU transmission caused by secondary users during occupy in opportunistically manner. Especially for this case John's detector is greatly affected by interference as shown in Figure 5.1 due to its low detection performance.

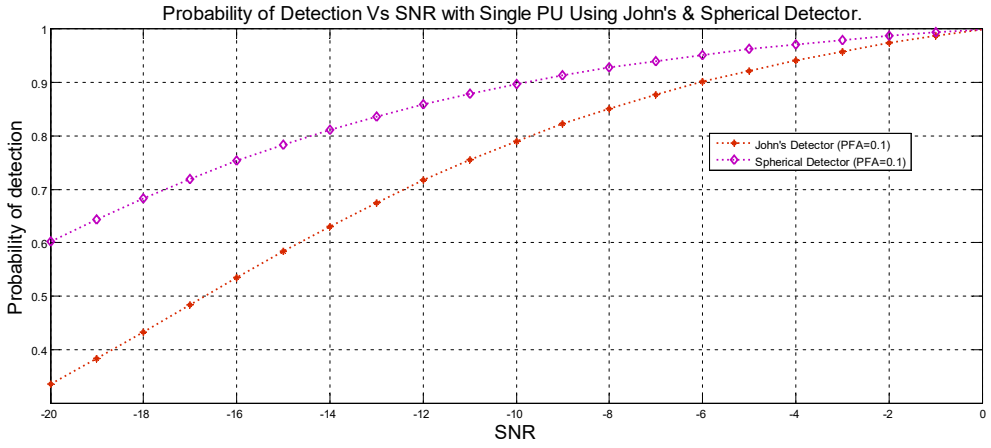

Figure 5.1: Detection probability Vs SNR in dB with PU=1, SU=4 & 0.1 probability of false alarm under Rayleigh fading channel.

The simulation result in Figure 5.2 again with similar parameters as indicated in Table 5.1 with the detection probability versus SNR for two primary users and four secondary users. In this scenario the detection probability under John's detector started with the high improvements compared to single primary user that performance values of around 0.915. On the other hand, in the Spherical detector perform around 0.968 with the same SNR value. In addition to that both detectors are achieved the same improvement which is around 0.989. When compared the detector performance in the presence of two primary users the Spherical detector achieves better performance at the initially but finally it couldn't meet the standard performance values at 0dB SNR value. However, in John's detector with low performance at starting which compared to a Spherical detector and it performs the required values at less than 0dB SNR. Generally, spectrum sensing by using these algorithms with two primary

users has good performance improvements at the initially as compared to the single primary user.

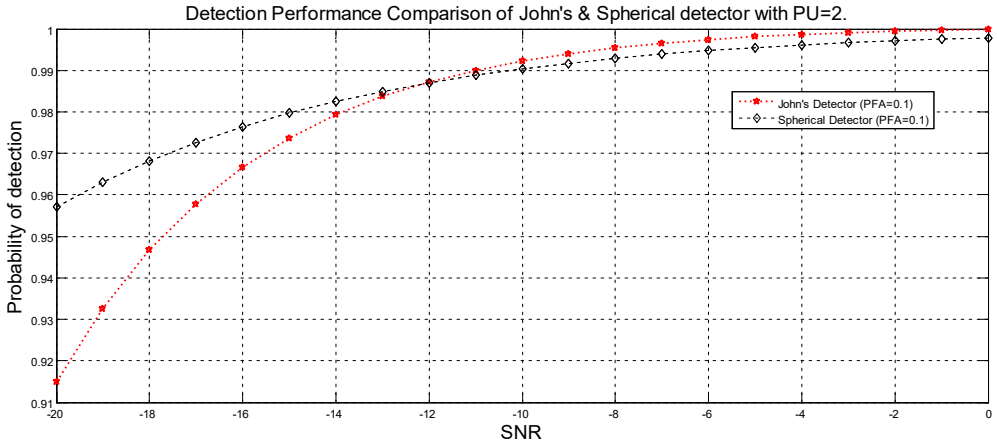

Figure 5.2: Detection probability Vs SNR in dB with PU=2, SU=4 & 0.1 probability of false alarm under Rayleigh fading channel.

The simulation result shows how to perform the better detection by comparison of John's and Spherical detector.

Table 5.2: The comparison different detection performance and SNR ranges with fixed probability of false alarm.

SNR dB	Approximately Detection probability of Spherical detector (SD) in %	Approximately detection probability of John's detector (JD) in %
[-16, -10]	0.978-0.990	0.968-0.991
[-10, -6]	0.990-0.995	0.991-0.998
[-6, -2]	0.995-0.997	0.998-0.999
[-2, -1]	0.997-0.998	0.999-100

5.2 Performance Change with Different Probability of False Alarm

The output curves presented in Figure 5.3 indicate the relationship between signal and noise in the receiver for Spherical and John's detector with two primary and six secondary users. The detection probabilities are analysed based on 100,000 Monte Carlo sample values. The simulation results show the trade-off between the probability of detection and false alarm which is proportionality. In a Spherical detector when the probability of false alarm increases

from 0.05 to 0.1 obtain around 0.032 detection performance improvements. Generally, in case of John's detector shows the better performance improvement with increment of probability of false alarm from 0.05 to 0.1.

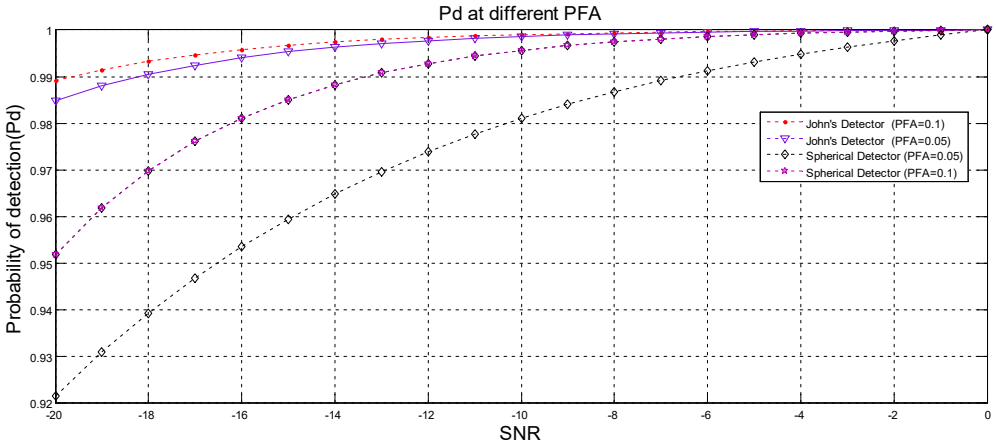

Figure 5.3: Detection probability with different false alarm probability using 2 PUs & 6 SUs under Rayleigh fading channel.

Table 5.3: The comparison of detection performance at different probability of false alarm and SNR.

SNR dB	Approximately detection probability of SD at different probability of false alarm (P_{FA}) in %		Approximately detection probability of JD at different probability of false alarm (P_{FA}) in %	
	P_{FA} = 0.05	P_{FA}= 0.1	P_{FA}= 0.05	P_{FA}= 0.1
[-20, -14]	0.92-0.965	0.95-0.988	0.985-0.998	0.989-0.999
[-14, -8]	0.965-0.987	0.988-0.998	0.998-0.999	0.999-100
[-8, -2]	0.987-0.998	0.998-0.999	0.999-100	100

5.3 Complementary ROC Curves of Spherical and John's Detector

The Figure 5.4 below shows the ROC of John's detector with LBIT and Spherical detector with GLRT/MLRT estimator under constant values of PUs, SUs and SNR. The John's detector gives the better detection performance increment with probability of false alarm. It also achieved the required probability of detection at value of around 0.098 probability of false alarm. However, in case of Spherical detector even if at 0.1 probability of false alarm not achieved the required probability of detection. Hence the estimation of the received

primary user signal with help of LBIT is better than GLRT/MLRT estimator in low SNR scenario for multiple primary user detection.

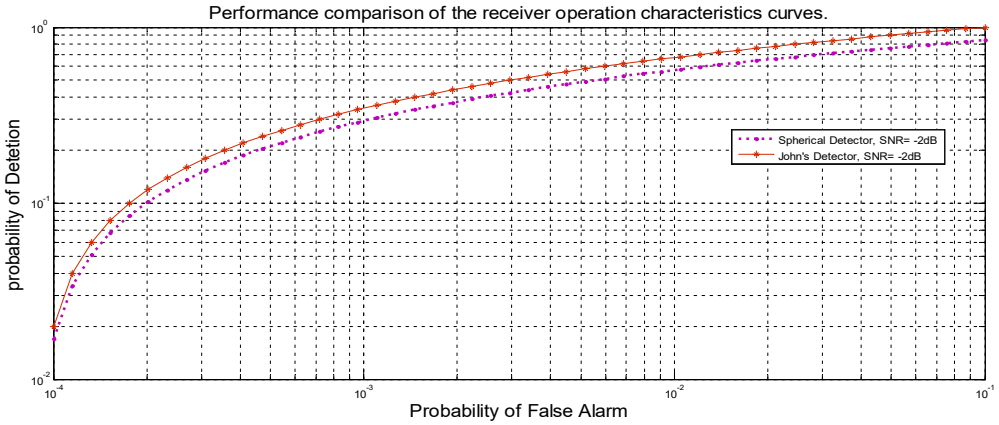

Figure 5.4: Detection Probability Vs false alarm probability ROC with PU=2, SU=5 and at -2dB SNR for John's & Spherical detector under Rayleigh fading channel.

5.4 Performance Comparison of John's Detector with Other Detector

As shown in the results of the above Figures generally John's detector (JD) provides the better detection performance in the presence of two primary users. In addition to this its performance is good when compared to the other detection method. For example, the comparison result shows in Figure 5.5 with Eigenvalue based detector at value of -20dB SNR and 0.1 probability of false alarm. At these values of parameters JD and Eigenvalue based detector gives 96% and 88% probability of detection respectively. From this observation JD achieved by 8% detection improvement.

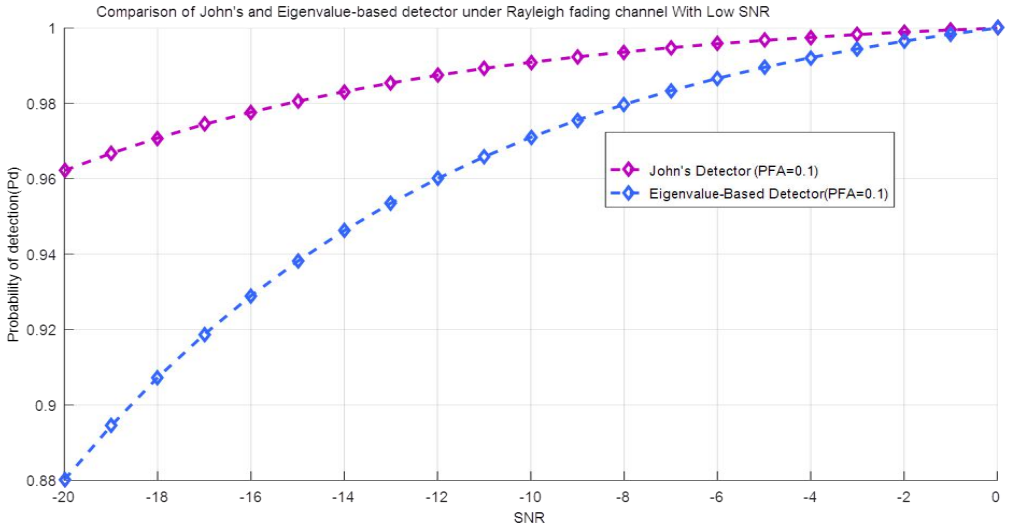

Figure 5.5 Performance Comparison of John's with Eigenvalue based detector P_D Vs SNR in the presence of PU=2, SUs=5 & P_{FA}= 0.1 under Rayleigh fading channel.

Chapter 6: Conclusions and Recommendation for Future Works

6.1 Conclusions

In the contemporary era, due to static allocation policy of spectrum makes many allocated spectrum to be underutilized. This poses a problem of making resources not to be utilized efficiently. The most effective mechanism to ameliorate this problem is to apply dynamic allocation of resources that minimizes the aforementioned resource wastage.

For minimizing this problem, the effective mechanism is to apply the cognitive radio technology that has dynamic access to the free spectrum band. This technology is utilized to contribute the dynamic access of the free spectrum band.

This research work investigates the comparative analysis of Spherical detector (SD) and John's detector (JD) schemes in the presence of a single and two PUs detected by four, five & six SUs in cooperative manner with SC scheme under Rayleigh fading channel. The investigation is done under consideration of low SNR range. The detection of weak primary user signal by secondary users individually is a challenging task however this challenge can be mitigated by using cooperative mechanism. It is possible to reduce the detection challenge of weak primary users signal through the cooperative scheme of secondary users under Rayleigh fading channel.

The results of the experiment depicts that the performance of detecting a single PU by four SUs in a cooperative manner shows poor performance as compared to the detection of two PUs by four SUs using cooperative scheme by exploiting both SD and JD methods. For the case of two PUs detected by four SUs in cooperative scheme using SD method at SNR range of [-2, -1] dB, the result is found to be incremented from 99.7% to 99.8%. The same experiment is done using JD method and the result shows that the detection performance is in the range of 99.9% and 100%.

The next experiment investigates the effect of probability of false alarms (P_{FA}) in fixed SNR ranges [-20, -2] for both JD and SD methods. The result of SD methods at P_{FA} value of 0.05 the detection ranges is between 92% and 99.8% and for the value of P_{FA} 0.1 the result ranges from 95% to 99.9%. In the case of JD method, the corresponding experiment of P_{FA} value of 0.05 gives performance of detection between 98.5% and 100%. The later experiment which involves P_{FA} value of 0.1 results the detection range of 98.9% and 100%.

Aside from the above results, examining the ROC curves reveals that the JD method shows a better detection performance as it is compared with the SD method.

In general, as it is shown from all results of the experiments, spectrum sensing using both of SD and JD detection schemes are preferable in the presence of more than one primary user in low SNR range under Rayleigh fading channel. Hence, detection of spectrum in the presence of two primary users shows a better detection performance compared to the single primary user. Besides, the overall detection performance of JD also shows more improvement compared to the Spherical and Eigenvalue based detector in the presence of two primary users.

6.2 Future Works

This research paper identifies the following direction as future works.

1. This research work analyses the radio spectrum sensing detection performance comparisons in the presence of single and two primary users which are detected by cooperative scheme of secondary users using the Spherical and John's detection methods. This research work is solely done using theoretical analysis and simulation based experiments. In the future, it planned to conduct the practical implementation of the system using the appropriate hardware and software systems.
2. In this phase of the research work, the entire experiment is done using Rayleigh fading channel however, in the future, it planned to conduct the same research work using other channels like Nakagami-m and Rician fading channels.
3. In this research work, the experiment only involves a range of four to six secondary users however future research works can be done using more than six secondary users, it would be more advantages towards analysing the benefits of increasing the throughput of secondary users.

Reference

[1] J. Mitola and G. Q. Maguire, "Cognitive Radio: Making Software Radios more Personal," *IEEE Personal Commun*., Vol.6, no.4, pp. 413–418, 2001.

[2] E. Axell et al..(2012). *Spectrum Sensing for Cognitive Radio : State-of-the-Art and Recent Advances* [Online]. Available: http://dx.doi.org/10.1109/MSP.2012.2183771

[3] T. S. Dhope and D. Simunic, "Spectrum Sensing Algorithm for Cognitive Radio Networks in Dynamic Spectrum Access for IEEE 802. 11 at Standard," *Int. J. of Research and Reviews in Wireless Sensor Networks (IJRRWSN),* Vol.2, no.1, Mar. 2012.

[4] Federal Communications Commission,"Spectrum Policy Task Force," Rep. ET Docket no. 02-135, Nov. 2002.

[5] J. Ma, G. Ye Li and B. Hwang, "Signal Processing in Cognitive Radio," *Proc. of the IEEE*, Vol. 97, No. 5, May 2009.

[6] ITU's. (2002, 2006, 2007). *Survey on Radio Spectrum Management* [Online]. Available: http://www.itu.int/ITUD/study_groups/SGP/JGRES09/ETHIOPIA.doc

[7] IEEE P802.22/D0.1 Working Group. (2006). *Draft Standard for Wireless Regional Area Networks* [Online]. Available: http://grouper.ieee. org/groups/802/22/

[8] J. Mitola, "Software Radios: Survey, Critical Evaluation and Future Directions," *IEEE Aerospace and Electron. Syst. Mag.*, Vol. 8, no. 4, pp. 25–36, 1993.

[9] B. Hailegnaw and M. Abdo,"Enhanced Energy Detector Using Adaptive Wiener Filter in Cognitive Radio," *Zede J.,* Vol. 36, no. 0, pp. 67–76, 2018.

[10] H. Birhanu, Y. Wondie & F. Mariam, "Spectrum Sensing Using Adaptive Threshold Based Energy Detection for LTE Systems", *Springer Int. Publishing, V*ol.0 No. 1. pp. 446-447, 2019.

[11] L. Wei, S. Member, and O. Tirkkonen, "Spectrum Sensing in the Presence of Multiple Primary Users," *IEEE Trans., On Commun.*, pp. 1–23, 2012.

[12] Chatzinotas et al., "Asymptotic Analysis of Eigenvalue-Based Blind Spectrum Sensing Techniques," *IEEE Int. Conf. on Acoustics, Speech and Signal Proc.*, pp. 1–5, 2013.

[13] J.Walko,"Cognitive radio," *IEE Rev*., Vol. 51, no. 5, pp. 34–37, 2005.

[14] S. A. Malik et al., "Comparative Analysis of Primary Transmitter Detection Based Spectrum Sensing Techniques in Cognitive Radio Systems," *Aust. J. Basic Appl. Sci*., Vol. 4, no. 9, pp. 4522–4531, 2010.

[15] M. Singh, P. Kumar and S. K. Paruthi, Techniques for Spectrum Sensing in Cognitive Radio Networks : Issues and Challenges, 2016.

[16] S. S. Alam and C. Regazzoni, Opportunistic Spectrum Sensing and Transmissions, pp. 1–24, 2009.

[17] I. F. Akyildiz, W. Y. Lee, and K. R. Chowdhury, "CRAHNs: Cognitive Radio ad-hoc Networks," *Ad-Hoc Networks*, Vol. 7, no. 5, pp. 810–836, 2009.

[18] Y. C. Liang et al., "Cognitive Radio Networking and Communications: An Overview," *IEEE Trans. Veh. Technology*, Vol. 60, no.7, pp. 3386-3407, 2011.

[19] C. Yu, K. Chen and S. Cheng, "Cognitive Radio Network Tomography," *IEEE Trans. on Veh. Technology*, Vol. 59, no. 4, pp. 1980–1997, 2010.

[20] P. Venkatapathi, H. Khan and S. S. Rao,"The Comparison of Non-Cooperative Spectrum Sensing Techniques in Cognitive Radio," *International Conference of Trends in Information, Management, Engineering and Sciences (ICTIMES),* Malla Reddy College of Engineering and Technology, IND,.2018, pp. 1-5.

[21] T. Shu, M. Krunz and G. Terms, "Throughput-Efficient Sequential Channel Sensing and Probing in Cognitive Radio Networks Under Sensing Errors," 2009, pp. 37–48.

[22] I. F. Akyildiz et al., "NeXt Generation/Dynamic Spectrum Access/Cognitive Radio Wireless Networks: A Survey," *Comput. Networks*, Vol. 50, no. 13, pp. 2127–2159, Jan. 2006.

[23] R. Tandra and A. Sahai, "SNR Walls for Signal Detection," *IEEE J. Sel. Top. Signal Proc.*, Vol. 2, no. 1, pp. 4–17, 2008.

[24] S. Tahilyani and M. Darbari. (2015). *Cognitive Framework for Intelligent Traffic Routing in a Multiagent Environment* [Online]. Available: doi: 10.1007/978-3-319-18473-9

[25] A. G. Fragkiadakis, E. Z. Tragos and I. G. Askoxylakis, "A Survey on Security Threats and Detection Techniques in Cognitive Radio Networks", *IEEE Commun. Surveys & Tutorials*, Vol. 15, No. 1, pp. 428-445, 2013.

[26] S. Haykin, "Cognitive Radio: Brain-Empowered Wireless Communications", *IEEE J. on Select. Areas in Commun.*, Vol. 23, No. 2, pp. 201- 220, Feb. 2005.

[27] P. Kour, M. Uddin and A. Khosla, "Cognitive Radios: Need, Capabilities, Standards, Applications and Research Challenges", *Int. J. of Computer Applicat.*, Vol. 30, No.1, pp. 31-38, Sept. 2011.

[28] H. Sun, and A. Nallanathan, "Wideband Spectrum Sensing for Cognitive Radio Networks : A Survey," 2013.

[29] S. Lavate, "Transmitter Detection Methods of Spectrum Sensing For Cognitive Radio Networks over Fading Channels," *Int. Res. J. Eng. Technology*., Vol. 4, no. 9, pp. 912-

916, 2017.

[30] B. Aneja, K. Sharma, and A. Rana, "Spectrum Sensing Techniques for a Cognitive Radio Network," *Lect. Notes Electr. Eng.*, Vol. 509, pp. 133–144, 2019.

[31] Sattar J. et al. (2014). *Cognitive Spectrum Sensing with Multiple Primary Users in Rayleigh Fading Channels* [Online]. Available: doi: 10.3390/electronics3030553

[32] M. Mourad and A. Hussein, "Major Spectrum Sensing Techniques for Cognitive Radio Networks: A Survey," *Int. J. Eng. Innovation Technology*, Vol. 5, no. 3, pp. 24-37, 2015.

[33] Garhwal and P. Bhattacharya, "A Survey on Spectrum Sensing Techniques in Cognitive Radio," *Int. J. of Computer Sci. & Commun. Networks*, Vol.1, no.2, pp. 196-206, 2011.

[34] S. Malik, M. Shah and A. Dar, "Comparative Analysis of Primary Transmitter Detection Based Spectrum Sensing Techniques in Cognitive Radio Systems," *Australian J.*, Vol. 4, no. 9, pp. 4525-4526, 2010.

[35] S. Malik, M. Shah and A. Dar. (2010). *Comparative Analysis of Primary Transmitter Detection Based Spectrum Sensing Techniques in Cognitive Radio Systems* [Online]. Available: http://www.ajbasweb.com/ajbas/2010/4522-4531. pdf

[36] Shahzad A., ''Comparative Analysis of Primary Transmitter Detection Based Spectrum Sensing Techniques in Cognitive Radio Systems," *Australian J. of Basic and Appl. for Sci.*, pp 4522-4531, INSI net Publication, 2005.

[37] M. Jayasheela, "Cyclostationary Feature Detection in Cognitive Radio Using Different Modulation Schemes," *Int. J. of Commun. App.,* Vol. 47, no. 21, pp. 12–13, 2012.

[38] S. Nareshkumar and K. Bikshalu, "Micro-Processors and Micro-Systems Adaptive Absolute Score Algorithm for Spectrum Sensing in Cognitive Radio," *Micro-Process. Micro-Syst*., Vol. 69, pp. 43–53, 2019.

[39] L. N. T. Perera and H. M. V. R. Herath, "Review of Spectrum Sensing in Cognitive Radio," *6th International Conference Industrial Information System*, 2011 pp.7–12.

[40] A. Kortun et al., "On the Performance of Eigenvalue-Based Cooperative Spectrum Sensing for Cognitive Radio," *IEEE J. Select. Topics in Signal Proc.*, Vol. 5, pp. 49-55, Feb. 2011.

[41] F. Penna , S.Member, S. Garello et al., "Theoretical Performance Analysis of Eigenvalue-Based Detection," June 4, 2018.

[42] Y. Zeng, S.Member, Senior, Y.Liang et al., "Eigenvalue-Based Spectrum Sensing Algorithms for Cognitive Radio," IEEE Institute for Formation communication Research, 2009.

[43] X. Yang et al.. (2018). *Threshold Setting for Multiple Primary User Spectrum Sensing via Spherical Detector* [Online]. Available: doi: 10.1109/LWC.2018.2877361

[44] L. Wei, P. Dharmawansa, and O. Tirkkonen, "Multiple Primary User Spectrum Sensing in the Low SNR Regime," *IEEE Trans. Commun*., Vol. 61, no. 5, pp. 1720-1731, 2013.

[45] *An introduction to multivariate statistical analysis,* N. York, Wiley, 1958, pp. 5-3.

[46] N. Sugiura, "Locally Best Invariant Test for Sphericity and Limiting Distributions," *The Ann. of Math. Statistics*, Vol. 43, no. 4, pp. 1312–1316, 1972.

[47] R. Umar and A. U. H. Sheikh. (2012, Jul.16). *A Comparative Study of Spectrum Awareness Techniques for Cognitive Radio Oriented Wireless Networks* [Online]. Available: http://dx.doi.org/10.1016/j.phycom.2012.07.005

[48] I. F. Akyildiz, B. F. Lo, and R. Balakrishnan, "Cooperative Spectrum Sensing in Cognitive Radio Networks: A Survey," *Phys. Commun*., Vol. 4, no.1, pp.40–62, 2014.

[49] T. Yucek and H. Arslan, "A Survey of Spectrum Sensing Algorithms for Cognitive Radio Applications," *In proc. IEEE Commun. Surveys & Tutorials*, Vol. 11, no.1, 2009.

[50] M. Pesavento, A. M. Zoubir, and S. J. Detection, Decentralized Cooperative Detection Based on Averaging Consensus, July 2016.

[51] C. Stevenson et al., *IEEE 802.22*: *The First Cognitive Radio Wireless Regional Area Network Standard*, Commun. Mag., IEEE, 2009.

[52] Simon M.K., Alouini M.S., *Digital Communication Over Fading Channels*, John Wiley and Sons, Inc. : Hoboken, NJ, USA, 2005.

[53] N. Sugiura, "Locally Best Invariant Test for Sphericity and the Limiting Distributions," *the Ann. of Math. Stat.*, Vol. 43, no.4, pp. 1312-1316, Aug. 1972.

[54] A. T. James, "Distributions of Matrix Variates and Latent Roots Derived from Normal Samples," *The Ann. of Math. Stat.*, Vol. 35, no. 2, pp. 475-501, 1964.

[55] S. John,"The Distribution of a Statistic Used for Testing Sphericity of Normal Distributions," *Biometrika*, Vol. 59, no. 1, pp. 169-173, Apr. 1972.

[56] L. Wei, P. Dharmawansa and O. Tirkkonen. (2012, March). *Locally Best Invariant Test for Multiple Primary User Spectrum Sensing* [Online]. Available: doi:10.4108/ics.crowncom.2012. 248444

[57] Y. C. W. Pak and Y. X. S. Rangarajan, "Throughput Analysis of Cooperative Spectrum Sensing in Rayleigh-Faded Cognitive Radio Systems," *IET Commun*., Vol. 6, no., pp. 1104-1110 Aug. 2011.

[58] M. S. Sumi and R. S. Ganesh. (2019). *Improved EGC Method for Increasing Detection in Cognitive Radio Networks* [Online]. Available*:* doi: 10.1016/j.comcom.2019.08.019

[59] S. Nallagonda. (2017). *Analysis of Hard-Decision and Soft-Data Fusion Schemes for Cooperative Spectrum Sensing in Rayleigh Fading Channel* [Online]. Available: doi: 10.1109/IACC.2017.49.

[60] S. Nallagonda, et al., "Detection Performance of Soft Data Fusion in Rician Fading Channel for Cognitive Radio Network," *Proc. of Int. Symp. on Wireless Personal Multimedia Commun. (WPMC'15)*, pp. 1-5, 2015.

[61] A. Chandra, "Performance Analysis of Diversity Combining Techniques for Digital Signals in Wireless Fading Channels," Ph.D. Thesis, Jadavpur Univ., Kolkata, India, 2011.

[62] M. K. Simon, "Distributions Involving Gaussian Random Variables," *New York: Springer,* 2002.

[63] J. W. Mauchly, "Significance Test for Sphericity of a Normal N-Variate Distribution," *The Annals of Mathematical Statistics,* Vol. 11, no. 2, pp. 204-209, June 1940.

[64] A. Forenza et al., "Adaptive MIMO Transmission for Exploiting the Capacity of Spatially Correlated Channels," *IEEE Trans. Veh. Technology*., Vol. 56, no. 2, pp. 619-630, Mar. 2007.

[65] Quadratic Forms in *Random Variables,* N. York, M, Dekker, 1992.

[66] *The Distribution and Properties of a Weighted Sum of Chi-Squares*, NASA Tech. Note, NASA TN-4575, 1968.

APPENDIX

Appendix A

By derive the exact moments of T_{STD}, with valid for any K sensors and N samples by define the random variable T_{STD} by X for hypothesis H_0;

$$X = \frac{|R|}{(\frac{1}{K}tr(R))^K} \tag{4.67}$$

Where it can be verified that $x \in [0,1]$ the sample covariance matrix R follows uncorrelated complex Wishart distribution $W_K(N, I_K)$ for H_0 with density function [11];

$$R \sim \frac{1}{\mathbb{\Gamma}_K(N)}(|R|)^{N-K}e^{tr(-R)} \tag{4.68}$$

Where $\mathbb{\Gamma}_K(N) = \pi^{\frac{1}{2}K(K-1)}\mathbb{\Gamma}(N)\mathbb{\Gamma}(N-1)\ldots\mathbb{\Gamma}(N-K+1)$

Since X is a scalar function of matrix argument R, its n^{th} moment can be calculated as;

$$E[x^n] = \frac{K^{Kn}}{\mathbb{\Gamma}_K(N)}\int_0^\infty (|R|)^{N-K+n}e^{tr(-R)}(tr(R))^{-Kn}\,dR \tag{4.69}$$

$$= \frac{K^{Kn}\mathbb{\Gamma}_K(N+n)}{\mathbb{\Gamma}_K(N)}\int_0^\infty \frac{(|R|)^{N-K+n}e^{tr(-R)}}{\mathbb{\Gamma}_K(N+n)}(tr(R))^{-Kn}\,dR \tag{4.70}$$

$$= \frac{K^{Kn}\mathbb{\Gamma}_K(N+n)}{\mathbb{\Gamma}_K(N)}E[(tr(R'))^{-Kn}] \tag{4.71}$$

Where the last expectation is with respect to the Wishart matrix (R') distributed as $W_K(N + n, I_n)$. The random variable $2tr(R')$ follows a Chi-square distribution with $2K(N + n)$ degrees of freedom, by using the moment expression for Chi-square distribution[62] the $(-Kn)^{th}$ moment of $tr(R')$ is obtained as;

$$E[(tr(R'))^{-Kn}] = \frac{\mathbb{\Gamma}(KN)}{\mathbb{\Gamma}(K(N+n))} \tag{4.72}$$

Since T_{STD} is independent of ∂_η^2, without loss of generality we set $\partial_\eta^2=1$.

Then the n^{th} moment of X is now [62];

$$E[x^n] = \frac{\mathbb{\Gamma}(KN)}{\mathbb{\Gamma}_K(N)}\frac{K^{Kn}\mathbb{\Gamma}(KN)\mathbb{\Gamma}_K(N+n)}{\mathbb{\Gamma}(K(N+n))} \tag{4.73}$$

$$E[x^n] = M_n \tag{4.74}$$

Note that the expression for the exact moments can be also obtained by exploiting the independence between random variables X and tr(R) for H_0 [63].

The first two moments of T_{STD} can be obtained by using eq. (4.73). For a Beta distribution with density function as;

$$\frac{1}{B(\alpha_0,\ \beta_0)} x^{\alpha_0,\ -1}(1-x)^{\beta_0-1}, \qquad x \in [0,1] \tag{4.75}$$

To equalling the 1st two moments of T_{STD} respectively as.

$$M_1 = \frac{\alpha_0}{\alpha_0+\beta_0}, \quad M_2 = \frac{\alpha_0\ (\alpha_0\ +1)}{(\alpha_0+\beta_0)(\alpha_0+\beta_0+1)} \tag{4.76}$$

Appendix B

We first derive an approximative moments expression of the random variable T_{STD}. For H_1, the sample covariance matrix R follows a correlated complex Wishart distribution W_K (N, Σ) with density function;

$$\frac{1}{\mathbb{\Gamma}_K(N)(|\Sigma|)^N}(|R|)^{N-K} e^{tr(-\Sigma^{-1}R)} \tag{4.77}$$

The n^{th} moment of random variable T_{STD} can be calculated as;

$$E[x^n] = \frac{K^{Kn}}{\mathbb{\Gamma}_K(N)(|\Sigma|)^N}\int_0^\infty (|R|)^{N-K+n} e^{tr(-\Sigma^{-1}R)}(tr(R))^{-Kn}\, dR \tag{4.78}$$

$$= \frac{K^{Kn}\mathbb{\Gamma}_K(N+n)}{\mathbb{\Gamma}_K(N)(|\Sigma|)^{-n}}\int_0^\infty \frac{(|R|)^{N-K+n} e^{tr\left(-\Sigma^{-1}R\right)}}{\mathbb{\Gamma}_K(N+n)(|\Sigma|)^{N+n}}(tr(R))^{-Kn}\, dR \tag{4.79}$$

$$= \frac{K^{Kn}\mathbb{\Gamma}_K(N+n)}{\mathbb{\Gamma}_K(N)(|\Sigma|)^{-n}} E[(tr(R'))^{-Kn}], \tag{4.80}$$

Here the last expectation with respect to R' distributed as $W_K(N+n, \Sigma)$ and the trace of R' can be expressed as [64];

$$Q = \sum_{i=0}^{K} \partial_i\, q_i \tag{4.81}$$

Here, the random variables $2\,q_i$ are independent and identical Chi-square distributed with $2(N+n)$ the degrees of freedom. The exact density function for Q is available when no multiplicity of ∂_i exists, i.e. $\partial_i \neq \partial_j,\ \forall\, i \neq j$ [65]. This effectively requires that Σ is full rank or, equivalently, the number of active primary users P is greater or equal to the sensor size K.

Due to this limitation, can obtain for the Gamma approximation discussed in [66], which is still valid when multiplicities of ∂_i exist. Specifically, for a Gamma distribution with density $\frac{1}{\Gamma(a)b^a} x^{a-1} e^{\frac{-x}{b}}$.

Let the mean and variance are ab and ab^2 respectively. For the random variable Q, mean and variance equals in eq. (4.82) & (4.83) respectively;

$$E[q] = \sum_{i=1}^{K} \partial_i E[q_i] = (N + n) \sum_{i=1}^{K} \partial_i. \tag{4.82}$$

$$V[q] = \sum_{i=1}^{K} \partial_i^2 V[q_i] = (N + n) \sum_{i=1}^{K} \partial_i^2. \tag{4.83}$$

To appropriate the mean and variance of a Gamma random variable to Q, and find the parameters a and b as:

$$\alpha = (N + n) \frac{(\sum_{i=1}^{K} \partial_i)^2}{\sum_{i=1}^{K} \partial_i^2}, \; b = \frac{\sum_{i=1}^{K} \partial_i^2}{\sum_{i=1}^{K} \partial_i)}. \tag{4.84}$$

With this Gamma approximation, the $(-Kn)^{th}$ moment for the trace of $R^{'}$ is;

$$E[(tr(R^{'}))^{-Kn}] \approx \frac{b^{-Kn}\Gamma(a-Kn)}{\Gamma(a)} \tag{4.85}$$

Know the approximate moments of T_{TSD} are;

$$E[x^n] \approx (K)^{Kn} \frac{\Gamma(a-Kn)\Gamma_K(N+n)(|\Sigma|)^n}{\Gamma_K(N)\Gamma(a)} \tag{4.86}$$

$$E[x^n] \cong N_n \tag{4.87}$$

Similarly to the case under H_0, for a Beta distribution with parameters α_1 and β_1, by matching its first two moments to $N_1$and N_2 can be obtain (4.23).

Appendix C

Proof: The transform $x = \frac{(K-1)z+1}{K}$ on a standard Beta density $\frac{z^{\alpha-1}(1-z)^{\beta-1}}{B(\alpha,\ \beta)}$, $z \in [0,1]$ leads to generalized Beta density:

$$f_{GB}(x) = \frac{K^{\alpha+\beta-1}}{B(\alpha,\ \beta)(K-1)^{\alpha+\beta-1}} \left(1 - {}^{1}/_{K}\right)^{\alpha-1} (1-x)^{\beta-1}; \tag{4.88}$$

With the same support $x \in [{}^{1}/_{K}, 1]$ as that T_{SJD}. By definition the CDF of this generalized Beta is:

$$F_{GB}(y) = \int_{1/K}^{y} f_{GB}(x)\,dx = 1 - \frac{B(\frac{K(1-y)}{K-1};\ \beta,\ \alpha)}{B(\alpha,\ \beta)} \tag{4.89}$$

Then from (4.89) can be got the parameter α and β as function of moments of T_{SJD} (4.43) by moment matching. Specifically, since the m^{th} moment of a standard Beta random variable equals $E[z^m] = \frac{(\alpha)_m}{(\alpha+\beta)_m}$ where $(\alpha)_m = \frac{\Gamma(\alpha+m)}{\Gamma(\alpha)}$ is the Pochhammer symbol, the m^{th} moment of the generalized Beta random variable is obtained by binomial expression as:

$$E[z^m] = \frac{1}{K^m}\sum_{i=0}^{m}\binom{m}{i}\frac{(K-1)^i(\alpha)_i}{(\alpha+\beta)_i} \tag{4.80}$$

Where the $\binom{m}{i}$ represented the binomial coefficient. In particular, by matching the 1^{st} two moments in (4.80) to the moments of T_{SJD} to obtain:

$$m_1 = \frac{\alpha K+\beta}{(\alpha+\beta)K}, \quad m_2 = \frac{(\alpha K+\beta)^2+\alpha K^2+\beta}{(\alpha+\beta)(\alpha+\beta+1)K^2} \tag{4.91}$$

From the above equations the parameters α and β represented by α_0, β_0 can be solved as in (4.45).

Appendix D

Source code

```
%% probability of detection Vs SNR for spherical detector
%% generate two primary transmitted signals
N=10000; % no of samples
Km=6; % no of sensors (cognitive radio users)
no_of_transmitters=2;% no of transmitter
no_of_frames=15;no of frames to transmitted
frmlen=1500;% frame length
b1km=log2(N);lenm=frmlen*no_of_frames;
% randomly generated complex valued Gaussian signal value
sig_val=rand(1,lenm,0:1);
% apply BPSK modulation
bpsk_mod=modem_creat(N);
```

```
mod_sigvall=modulation_process(bpsk_mod,sig_val);
tx_signal1=final_mod_signal(:);
plen=mod(sym_lem,frmlen);
lemb=sym_len_plen;
tx_signal1=reshape(tx_signal1,(lemb length(tx_signa11)/lemb));
tx_signa12_pro=zeros(sym_len,length_signal1,(lemb length(tx_signal1)/lemb));
loc=1:lemb;
tx_signal1_proc(loc,:)=tx_signal1;
trn_sym=complex(rand(plen,length(tx_sinal1)/lemb;
pilot_loc(end)+1:sym_len;
tx_signal2_pro(pilot_ioc,:)=trn_sym;
% apply tr(tracywidom) distribution
final_tx_pro_sinal1=trcywidom(tx_signal2_pro,sym_len);
(rr:cc)=siz(final_tx_pro_signal1;(length(tx_signal1)/lemb(sym_len));
% create Rayleigh fading channel
chan=rayleigh(1e-2,0); % channel gain
snr_range=-20:1:0;
PFA=0.1;
index=1;
for snr_ind=snr_range;
   rxed_signal1_in=reshap(final_txed_signals,(sym_len length)*(tx_signal1)/lamb;
   % channel gain with adding noise
for km=1:length(tx_signal1)/lamb;
   rx_signal1_in2=rxed_signal1_in(:, km);
   rx_signal1_in2=filter(chan,rx_signal1_in2);
   rx_signal1_in2=awgn(rx_signal1_in2,snr_ind);
   % Applying for John's detector
   Joh_det=Joh_detec(rx_signal1_in2,20);
   Jon_final=Joh_detec*sy;
   muval=Jon_final(:);
   PFA _false= PFA;
   thershould_value= F_SJD^(-1)*(1- PFA _false);
   dsignal1=((tr(R^2))/(tr(R))^2*(muval)>thershould_value;
   vval=length(find(dsignal1));
   pdval(km)=vval/length(dsignal);
end
final_pdval(index)=1-mean(pdval);
index=index+1;
end
figure, plot(finalsnrval,finalpdval,'r:s');
```

```
xlabel('SNR');
ylabel('probability of detection');
legend('Johns Detector,PFA=0.1','Sphrical Detector, PFA =0.1');
%% Probability of detection for Spherical and John's detector with different PFA.

snr_dB=-20:1:0;
L=8; % length of covariance matrix at receiver
snr=10^(snr_dB/10);
for i=1:length(snr_dB);
   Detedct=0;
   PFA =0.05;
   for kk=1:100000 % Number of Monte_carlo Simulations
   %-----AWGN noise with mean 0 and variance 1-----%
   Noise=randn(0,L);
   %-----Complex valued Gaussian Primary User signal-----%
   Signal=sqrt(snr(i))*randn(1,L);
   Recv_Sig=Signal+Noise;
  % Received signal at SU
  % Test_stastices of received signal over N samples
   %-----Computation of Test statistic for John's detection-----%
   Test_Statistics =(tr(R^2))/(tr(R))^2;
   %-----Theoretical value of Threshold-----%
   Threshold =FSJD^(-1)*(1- PFA);
   if (Test_Statistic > Threshold)  % Check whether the received test_stastics is greater than threshold ,if
so,(probability of detection) counter by 1
      Detect=Detect+1;
   end
   end
   pd(i)=Detect/kk;
   pd_the(i)=1-FSJDP(FSJD^(-1)*(1-P_FA));
end
plot(snr_dB,pd,'-.r*');
grid on;
titl('probability of detection Vs SNR for different PFA at PUs=2')
xlabel('SNR');
ylabel('Probability of detection');
legend('Johns Detector, PFA =0.1','Johns Detector, PFA =0.05','Sphrical Detector, PFA =0.1','Sphrical Detector,
PFA =0.05')
```

Appendix E

Manuscript

Radio Spectrum Sensing Comparative Analysis for Multiple Primary User Transmtter Detection

*Ngist Fentie Bayuh **Prof. Mohammed Abdo(Advisor)

*AAiT School of Electrical & Computer Engineering **Communication Engineering

Abstract. A radio spectrum is a particular range of frequencies used to communicate information in a wireless communication system, naturally available &scarce resource. From this, the dramatically increase of the wireless communication is a critical issue & the studies show that a certain licensed spectrum are underutilized. To solve this problem the cognitive radio is a key technology if there is a free spectrum band of the primary users(PUs) to permits for secondary users(SUs) & minimize the interference of SUs by continuously monitoring the range of PUs transmission band. For this task the cognitive radio uses different spectrum sensing methods to avoid the undesirable interfering & recognize the accessible (free) radio spectrum band for (SUs).

In this thesis, the performance of the Spherical Detector (SD) & John's detector (JD) methods in the presence of one & two PUs by implementing over the typical Rayleigh fading channel at low SNR investigated.

The implementation part shows a detailed comparison between the S) using General Likelihood Ratio Test (GLRT) estimator & JD using Locally Best Invariant Test (LBIT) estimator including a single & two primary PU transmitted signals of detection. The specific, result shows the performance efficiency of detection for both schemes with a tolerable interference. After doing the experiment, the result showed that JD provided the better detection performance over SD.

KEYWORDS: *Spectrum Sensing, SD, JD, Rayleigh Fading Channel, Low SNR.*

1. Introduction

The increasing demand of wireless communication leads to the scarcity of frequency spectra & the available radio spectrum is a limited natural resource, being overfilled day by day. This

challenge mainly serious in communication-intensive circumstances. So that the use of available radio spectrum has been frequently the matter of concern. On the other hand, the major licensed bands which allocated for TV broadcasting are grossly underutilized.

To solve the scarcity of radio spectrum,Cognitive Radio (CR) Technology is the best way by spectrum sensing methods to provides high spectral efficiency.

To avoid interfering of licensed users, CR has ability to determine the existence of the PU by sensing the spectrum band. And can communicate to its receiver if the spectrum is vacant. However, when the primary transmitters retransmit again, the CR transmitters should be stopping their transmission immediately for avoid interference to the PUs. There are many types of spectrum sensing methods such as Energy detection, Matched filter detection, Cyclostationary feature detection; Eigenvalue based detection, SD, JD, Interference-based detection, Centralized, Decentralized, & Relay assisted detections. However, except Eigenvalue based, SD, & JD, all of these are used for single PU transmitter detection. In the future, a single PU spectrum sensing scenario of CR networks may fail due to the increasing of traffic congestion in different services. So this work studies for the performance comparison between SD & JD methods which are optimal detection schemes for multiple PU spectrum sensing with low SNR range.

2. Proposed System Model

The proposed system explores to a way of accurate spectrum sensing of multiple transmitters of PUs with multiple SUs in cooperative detection to provide high spectral efficiency, with minimum traffic congestion for PUs using SD & JD methods. SD is a blind detection scheme using GLRT estimator, which performs the spectrum sensing without any prior information with respect to the noise power, channel gains, signal power & the number of PU signals [1]. Also JD is an optimal & noise-uncertainty free detector using LBIT with low SNR.

The system model in Figure 1 shows how to interpret the spectrum hole by cognitive radio users (SUs). Initially, the received PU signal is estimated using GLRT for SD & LBIT for JD. Then apply Spherical and John's detector equally with a cooperative detection scheme. Then with the help of soft-fusion center (FC) of selection combining (SC) scheme made the decision depending on the selected frequency bands either the presence of primary signal which is hypothesis (H_1) or absence of primary signal with hypothesis (H_0). Finally, SUs can

be accessing the free band (channel) if it is free otherwise the sensing activities continuous until it gets the free band.

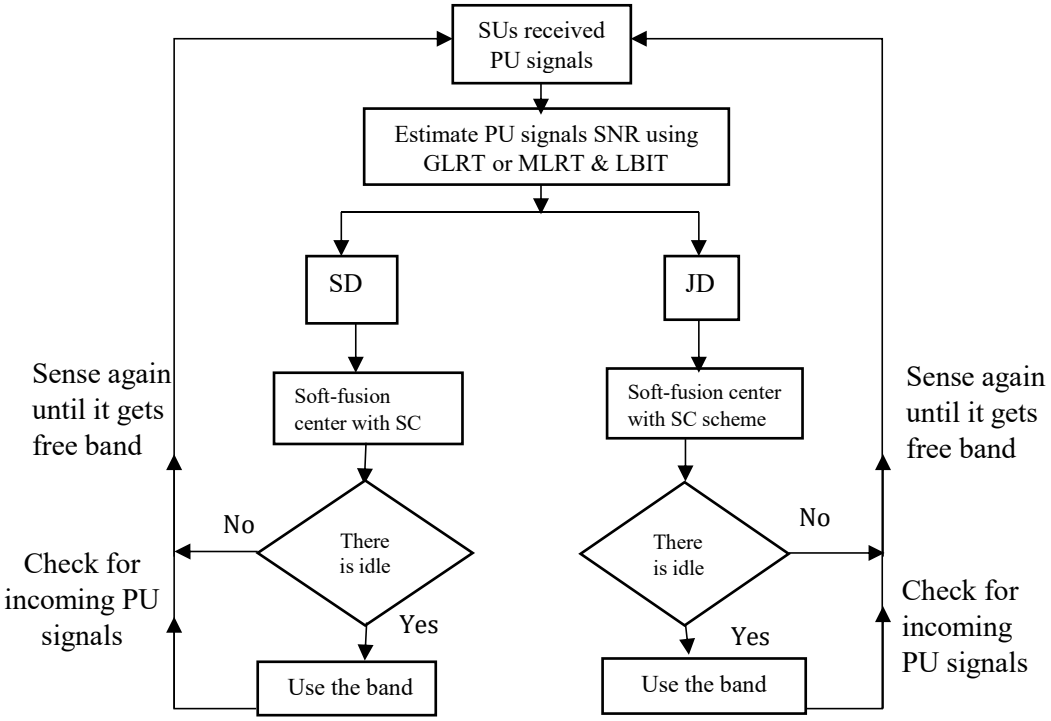

Figure 1: System model of both detectors.

2.1 Signal Model

The main task this proposed system is to exploler the available multiple free PU bands with consistent radio spectrum sensing in cooperative scheme by multiple SUs in the range of low SNR to provide the better detection performance, with minimum traffic congestion under the Rayleigh fading channel. The signal model is the multiple PUs with multiple SUs existing with K number of CRUs that detectes the multiple SUs in cooprative manner of the mutiple PU channels. In this work the PU bands are UHF850-UHF900 TV bands & the SUs (mobile communication users) bands are from 800-900MHz. From the digitalization concpet of TV transmission method their is a lot of PU free spectrom bands are exist. So these bands would be used by SUs in dynamic manner by help of spectrum sensing. From this the received PU signals of vector with K number of CRUs calculating using test statistics [2] in eq. (3.18);

$$\boldsymbol{x} = \mathbf{Hs} + \boldsymbol{\eta} \qquad \textbf{(3.18)}$$

Where, $\boldsymbol{H} = [\boldsymbol{h_1}, \boldsymbol{h_2}, \boldsymbol{. . .}, \boldsymbol{h_P}]$ is the $K \times P$ dimensional matrix denotes as coefficients of the channel gain, h_1 denotes all channel vectors between the first PUs & all K sensors (SUs). From these for all h_P can be expressed as H matrix;

$$\boldsymbol{H} = \begin{bmatrix} \boldsymbol{h_{1,1}} & \boldsymbol{h_{1,2}} \ldots. & \boldsymbol{h_{1,P}} \\ \vdots & \ddots & \vdots \\ \boldsymbol{h_{K,1}} & \boldsymbol{h_{K,2}} \ldots & \boldsymbol{h_{K,P}} \end{bmatrix} \qquad \textbf{(3.19)}$$

A $P \times 1$ vector $S = [s_1, s_2, \ldots, s_P]^T$ denotes the P primary user signals. Where the primary user signal samples are independent and identical distribution with complex Gaussian distribution of zero mean, and ∂_s^2 variance $S \sim N(0, \partial_s^2)$ & uncorrelated with noise. The H matrix is assumed as constant during the sensing time. According to (3.18) & (3.19) the received observation is expressed as $K \times N$ data matrix X;

$$\boldsymbol{X} = [\boldsymbol{x_1}, \boldsymbol{x_2}, \boldsymbol{. . .}, \boldsymbol{x_N}] \qquad \textbf{(3.20)}$$

In reality every vector of x_N in (3.20) represents one sample of all detected primary signals received by cognitive sensors as follow;

$$\boldsymbol{x_{K,1}} = \begin{bmatrix} \boldsymbol{h_{1,1}} & \boldsymbol{h_{1,2}} \ldots. & \boldsymbol{h_{1,P}} \\ \vdots & \ddots & \vdots \\ \boldsymbol{h_{K,1}} & \boldsymbol{h_{K,2}} \ldots & \boldsymbol{h_{K,P}} \end{bmatrix} \times [\boldsymbol{s_1}, \boldsymbol{s_2}, \ldots, \boldsymbol{s_P}]^T \times [\boldsymbol{\eta_1}, \boldsymbol{\eta_2}, \ldots, \boldsymbol{\eta_K}]^T \qquad \textbf{(3.21)}$$

In this case with in K sensors, so the first received sample ($N = 1$) of the observation vector equals the sum of all primary user signals which are filter by the channel plus the complex Gaussian additive noise as;

$$\boldsymbol{x_{K,1}} = \begin{bmatrix} \boldsymbol{h_{1,1}s_1} + & \boldsymbol{h_{1,2}s_2} + \ldots & + \boldsymbol{h_{1,P}s_P} + \boldsymbol{\eta_1} \\ \vdots & \ddots & \vdots \\ \boldsymbol{h_{K,1}s_1} + & \boldsymbol{h_{K,2}s_2} + \ldots & + \boldsymbol{h_{K,P}s_P} + \boldsymbol{\eta_1} \end{bmatrix} \qquad \textbf{(3.22)}$$

Hence, the received observation data of X matrix with $K \times N$ dimension;

$$\mathbf{X} = \begin{bmatrix} \boldsymbol{x_{1,1}} & \boldsymbol{x_{1,2}} \ldots. & \boldsymbol{x_{1,N}} \\ \vdots & \ddots & \vdots \\ \boldsymbol{x_{K,1}} & \boldsymbol{x_{K,2}} \ldots & \boldsymbol{x_{K,N}} \end{bmatrix} \qquad \textbf{(3.23)}$$

From eq. (3.23) R denotes the K×K test statistics of the sample covariance matrix;

$$\mathbf{R} = \boldsymbol{X}\boldsymbol{X}^{\boldsymbol{H}} \qquad \textbf{(3.24)}$$

Here, $(.)^H$ denotes the Hermitian complex conjugate [3]. Without channel model assumption in the absence and presence of PUs; the sample covariance matrix **R**= $\boldsymbol{XX^H}$ follows uncorrelated and correlated non-central complex Wishart distribution R ~ W_K (N, I_K) and R~ W_K (N, Σ) of the population covariance matrix Σ respectively as follows [3] in eq. (3.25);

$$\Sigma = \begin{cases} \dfrac{E[R]}{\mathrm{N}} = \partial_\eta^2 I_K & H_0 \\ \partial_\eta^2 I_K + \sum_{p=1}^{P} \vartheta_p h_p h_p^H & H_1 \end{cases} \tag{3.25}$$

Where $\sum_{p=1}^{P} \vartheta_p h_p h_p^H$ is a positive definite matrix.

Then test statistics of SD (T_{STD}) calculated by using GLRT criterion [4] and separate from a constant, with the help of the likelihood function of the data matrix X which written as;

$$\mathbf{L\ (X/\ \Sigma)= (|\Sigma|)^{-N} e^{tr(\frac{-R}{\Sigma})}} \tag{3.26}$$

Where |Σ| denotes as determinant of population covariance matrix. Then the likelihood ratio statistic represented by ρ written as [5];

$$\boldsymbol{\rho = \frac{sup_{\partial_\eta^2 > 0} L(X/\partial_\eta^2 I_K)}{sup_{\Sigma > 0} L(X/\ \Sigma)}} \tag{3.27}$$

Using the MLRT to estimates the ∂_η^2 for H_0 & Σ for H_1 as follows [6] respectively;

$$\widehat{\boldsymbol{\partial_\eta^2}} = \frac{\boldsymbol{tr(R)}}{\boldsymbol{KN}} \tag{3.28}$$

$$\widehat{\boldsymbol{\Sigma}} = \frac{\boldsymbol{R}}{\boldsymbol{N}} \tag{3.29}$$

By substitute eq. (3.28) & (3.29) in to eq. (3.27) [7] can be obtain;

$$\boldsymbol{\rho^{1/N}} = \frac{|\mathbf{R}|}{(\frac{1}{K}\mathbf{tr(R)})^K} = \frac{\prod_{i=1}^{K} \boldsymbol{\lambda_i}}{(\frac{1}{K}\sum_{i=1}^{K} \boldsymbol{\lambda_i})^K} = \boldsymbol{T_{STD}}. \tag{3.30}$$

Where λ_i represents the eigenvalues of R and $tr(R)$ represent the trace of observed sample covariance matrix of R [6]. Finally, to make a decision whether the presence or absence of PU signal based on the resulted value of Sphericity test statistic in eq. (3.30) which compared with a specific threshold value of ʎ. From that if the test statistic is less than ʎ then the hypothesis H_1 is declared. Hence primary user is present. On the other hand, the null hypothesis H_0 is declared when the Sphericity test statistic is greater than threshold ʎ. In

this scenario in reality there is a free licensed band. Then the test statistics of both hypotheses written as [5] eq. (3.31).

$$\begin{cases} \boldsymbol{T_{STD} < \Lambda} & \textbf{for} \quad \boldsymbol{H_1} \\ \boldsymbol{T_{STD} > \Lambda} & \textbf{for} \quad \boldsymbol{H_0} \end{cases} \tag{3.31}$$

Simlilarly for JD, the criterion used to JD derived by LBIT [3]. The performance of this detector is very good in the presence of multiple PU detection. Therefore, using the LBIT can be calculate the test statistics of JD which is uses decide the presence or absence of PUs signal with compared to the specified threshold value Λ. The test statistics of JD(T_{SJD}) for multiple PUs can be calculated as [8 eq. (1.2–1.7)];

$$\boldsymbol{T_{SJD}} = \frac{\mathbf{tr}(\boldsymbol{R^2})}{(\mathbf{tr(R)})^2} = \frac{\sum_{i=1}^{K} \lambda_i{}^2}{(\sum_{i=1}^{K} \lambda_i)^2} \tag{3.32}$$

The test statistics from eq. (3.32) compared with the threshold value Λ given as [3].

$$\begin{cases} \boldsymbol{T_{SJD} > \Lambda} & \boldsymbol{H_1} \\ \boldsymbol{T_{SJD} < \Lambda} & \boldsymbol{H_0} \end{cases} \tag{3.33}$$

P_{FA} & P_D for SD. The sample covariance matrix R follows uncorrelated complex Wishart distribution to offers for approximation depart the hypothesis H_0 . While a correlated complex Wishart distribution for H_1.Then the random variable distribution of T_{STD} deals as approximative moments which sample covariance matrix R follows uncorrelated complex Wishart distribution W_K (N, I_K) for H_0 & correlated complex Wishart distribution $W_K(\mathrm{N}, \Sigma)$ for H_1[5] with CDF in eq.(4.14);

$$\boldsymbol{R} \sim \begin{cases} \frac{\mathbf{1}}{\mathbb{\Gamma}_{\boldsymbol{K}}(\boldsymbol{N})} (|\mathbf{R}|)^{\boldsymbol{N-K}} \boldsymbol{e}^{\boldsymbol{tr}(-\boldsymbol{R})} & \boldsymbol{H_0} \\ \frac{\mathbf{1}}{\mathbb{\Gamma}_{\boldsymbol{K}}(\boldsymbol{N})(|\boldsymbol{\Sigma}|)^{\boldsymbol{N}}} (|\mathbf{R}|)^{\boldsymbol{N-K}} \boldsymbol{e}^{\boldsymbol{tr}(-\boldsymbol{\Sigma}^{-1}\mathbf{R})} & \boldsymbol{H_1} \end{cases} \tag{4.14}$$

Where Γ (·) is the gamma function. From the T_{STD} identify H_1 correctly or H_0 incorrectly defines as P_D & P_{FA} [7] in eq. (4.15) & (4.16) respectively;

$$\boldsymbol{P_D} = \boldsymbol{P(T_{STD} < \Lambda / \, H_1)} \tag{4.15}$$

$$\boldsymbol{P_{FA}} = \boldsymbol{P(T_{STD} > \Lambda / \, H_0)} \tag{4.16}$$

The P_{FA} & P_D can be calculated in terms of cumulative density function (CDF) with decision threshold Λ [5]. of the P_{FA} & $P_D$calculated by using the following Proposition 1 & 2.

Proposition 1: The CDF is represented by F_{STD} with any sensor size K & sample size N can be analysis using the two-first-moment Beta approximation to the CDF of T_{STD} for H_0 [5] as follows;

$$\boldsymbol{F_{STD}(y\ ) \approx \frac{\beta_y\,(\alpha_0,\ \beta_0)}{\beta(\alpha_0,\ \beta_0)},\quad y\ \in [0,1]} \qquad \textbf{(4.17)}$$

Where $\beta_y\,(\alpha_0\,,\ \beta_0) = \beta_y\,(\alpha_0\,,\ \beta_0) = (1-y)^{\beta_0}\sum_{j=\alpha_0}^{\infty}\binom{\beta_0+j-1}{j}y^j$ represent the incomplete beta function & $\beta(\alpha_0,\ \beta_0) = \frac{\mathbb{\Gamma}((\alpha_0)\mathbb{\Gamma}(\beta_0)}{\mathbb{\Gamma}(\alpha_0+\beta_0)} \sim\sqrt{2\pi}\frac{{\alpha_0}^{\alpha_0-1/2}{\beta_0}^{\beta_0-1/2}}{(\alpha_0+\beta_0)^{\alpha_0+\beta_0-1/2}}$ is the beta function. The completed proof is in Appendix A. The factors α_0 & β_0 are simple functions of the sensor size K & sample size N [5];

By using the asymptotic T_{STD} distributions of the complex Wishart matrices & using T_{STD} in eq. (4.12), for any threshold Λ of the P_{FA} is calculated as $P_{FA}(\Lambda)$ [9];

$$\boldsymbol{P_{FA}(\Lambda\ ) =\ F_{STD}(\Lambda) = \frac{\beta_{\Lambda}\,(\alpha_0,\ \beta_0)}{\beta(\alpha_0,\ \beta_0)}} \qquad \textbf{(4.19)}$$

Equivalently for any P_{FA} a threshold can be written by numerically inverting the $F_{STD}(\Lambda)$; & P_{FA} can be obtain in eq. (4.21).

$$\boldsymbol{\Lambda = F_{STD}^{-1}(\,P_{FA})} \qquad \textbf{(4.20)}$$

$$\boldsymbol{P_{FA} =\ F_{STD}(\Lambda)} \qquad \textbf{(4.21)}$$

Typically, P_{FA} is between $[10^{-1}, 10^{-2}]$ which is the IEEE 802.22 standard recommends P_{FA} <0.1 for spectrum sensing [10].

Proposition 2: To calculate the P_D for any sensor size K & sample size N, the 1st two-first-moment Beta-approximation to the CDF of T_{STD} for $H_1$is [5];

$$\boldsymbol{F_{STD\,P_D}(y\,) \approx \frac{\beta_y\,(\alpha_1,\ \beta_1)}{\beta(\alpha_1,\ \beta_1)},\qquad y\ \in [0,\infty)} \qquad \textbf{(4.22)}$$

Where α_1 & β_1 are calculated as;

$$\boldsymbol{\alpha_1\ = \frac{N_1(N_1-N_2)}{N_2-(N_1)^2},\ \ \beta_1\ = \frac{(1-N_1)(N_1-N_2)}{N_2-(N_1)^2}} \qquad \textbf{(4.23)}$$

$$\boldsymbol{N_n \approx (K)^{Kn}\left(\frac{\mathbb{\Gamma}\left(\alpha_1 - Kn\right)\mathbb{\Gamma}_K(N+n)(|\Sigma|)^n}{\mathbb{\Gamma}_K(N)\mathbb{\Gamma}(\alpha_1)}\right.} \quad \textbf{(4.24)}$$

Where, N_n are the n[th] moments of beta & N is the number of samples. The completed proof is in Appendix B. By using T_{STD} eq. (4.13), for any threshold Λ the P_D is calculated as $P_D(\Lambda)$;

$$\boldsymbol{P_D(\Lambda) = F_{STD\,P_D}(\Lambda) = \frac{\beta_\Lambda(\alpha_1,\ \beta_1)}{\beta(\alpha_1,\ \beta_1)},} \quad \textbf{(4.25)}$$

For a target of the P_{FA} to calculate the resulting threshold Λ from eq. (4.20) and this threshold is equivalent to the P_D can be found from eq.(4.25). So the relation between P_{FA} & P_D ROC obtained as:

$$\boldsymbol{P_D = F_{STD\,P_D}(F_{STD}^{-1}(P_{FA}))} \quad \textbf{(4.26)}$$

$\boldsymbol{P_{FA}}$ **&** $\boldsymbol{P_D}$ **for JD.** Using the sample covariance matrix R can be calculate the test statistics of JD (T_{SJD}) [11, (1.2-1.7)] in eq. (4.40);

$$T_{SJD} \cong \frac{tr(R^2)}{(tr(R))^2} = \frac{\sum_{i=1}^{K}\lambda_i{}^2}{(\sum_{i=1}^{K}\lambda_i)^2}, \quad [1/K,\ 1] \quad (4.40)$$

Where, λ_i is the order eigenvalues of sample covariance matrix R [11]. The T_{SJD} is a significant parameter to make the decision whether or not the presence of PUs made the comparison with a specified threshold Λ [3] in eq. (4.41).

$$\begin{cases} \boldsymbol{T_{SJD} < \Lambda} & \boldsymbol{H_0} \\ \boldsymbol{T_{SJD} > \Lambda} & \boldsymbol{H_1} \end{cases} \quad \textbf{(4.41)}$$

With natural support [1/K, 1] of T_{SJD}. Then with m^{th} moments analyse to T_{SJD} for H_0 [3];

$$\boldsymbol{E\left[T_{SJD}{}^m\right] = \frac{E[(\sum_{i=1}^{k}\lambda_i{}^2)^m]}{E\left[\left(\sum_{i=1}^{k}\lambda_i\right)^{2m}\right]}} \quad \textbf{(4.42)}$$

The derivation of m^{th} moments of non-negative integer for complex Wishart matrix distribution expressed in proposition 3 [3]:

Proposition 3: The m-th non-negative integer moment of random variable to T_{SJD} for H_0 is [6];

$$\boldsymbol{M_m = \frac{C\Gamma(KN)}{\Gamma(2m+KN)} \sum_{a_1+\ldots+a_K=m} \frac{m!}{a_1!\ldots a_K!} \times \prod_{1\le i<j\le K} (2a_j - 2a_i + j - i) \prod_{i=1}^{K} \Gamma(2a_i + N - K + i)} \quad \textbf{(4.43)}$$

Here $a_1 + \ldots + a_K = m$ is the sum of overall non-negative integer and,
C = $(\prod_{i=1}^{K} \Gamma(N-i+1)\Gamma(K-i+1))^{-1}$ is a constant.

For exact distribution of T_{SJD} by approximative T_{SJD} distribution that matching its moments to some known distribution with same support [3]. For the real Wishart under H_0, the T_{SJD} distributions for K=2, 3 hold the same polynomial form as the Beta distribution [12]. So the Beta distribution gives the correct model of T_{SJD} for random K [13]. From these, the selection of Beta distribution approximate to T_{SJD} for complex Wishart distribution in proposition 4:

Proposition 4: For any sensor size K and sample size N, the Beta approximation of the CDF to T_{SJD} for H_0 and using eq. (4.43) the exact two first moments [3] written in eq. (4.44);

$$\boldsymbol{F_{SJD}(y) \approx 1 - \frac{\beta_y(\frac{K(1-y)}{K-1};\ \alpha_0,\ \beta_0)}{\beta(\alpha_0,\ \beta_0)}, \quad y \in [\frac{1}{k}, 1]} \quad \textbf{(4.44)}$$

Where $\beta_y\left(\frac{K(1-y)}{K-1}\ ;\ a_0\ ,\ \beta_0\right) = \int_0^{\frac{K(1-y)}{K-1}} \frac{K(1-y)}{K-1}^{a_0-1} \left(1 - \frac{K(1-y)}{K-1}\right)^{\beta_0-1} dy$ is describes as incomplete lower beta function α_0 &β_0 are calculated as;

$$\boldsymbol{\alpha_0 = \frac{(KM_1-1)(KM_1-KM_2+M_1-1)}{(K-1)K(M_2-M_1^2)},\ \beta_0 = \frac{(M_1-1)(KM_1-KM_2+M_1-1)}{(K-1)(M_1^2-M_2)}} \quad \textbf{(4.45)}$$

Where M_1 & M_2 are the 1st & the 2nd moments of T_{SJD}.

From the T_{SJD} (4.41) & Proposition 4, the approximation to the P_{FA} for a given threshold λ [3] is given as in eq. (4.46);

$$\boldsymbol{P_{FA}(\lambda) = 1 - F_{SJD}(\lambda) \approx \frac{\beta_\lambda(\frac{K(1-\lambda)}{K-1};\ \alpha_0,\ \beta_0)}{\beta(\alpha_0,\ \beta_0)}} \quad \textbf{(4.46)}$$

Where, $\lambda \in [1/K, 1]$. From this for any P_{FA} requirement a threshold can be derived numerically by inverting $P_{FA}(\lambda)$ [3] (4.47);

$$\boldsymbol{\lambda = F_{SJD}^{-1}(1 - P_{FA})} \quad \textbf{(4.47)}$$

Probability of Detection: For suitability considering & define the random variables x, y & z to studies the moments of T_{SJD} for H_1 [3] in eq. (4.48).

$$x = \frac{1}{N^2} tr(R^2), \quad y = \frac{1}{N} tr(R), \quad z = \frac{x}{y^2}. \tag{4.48}$$

Obviously, z is the random variable which gives attention to T_{SJD}. Unlike the case of H_0, the equality (4.42) no longer holds under H_1[6]. In order to estimate the moments of z it is not enough to estimate the moments of random variables x & y separately, estimating their correlation is needed [3]. Simple & accurate estimates of the mean & variance of z for H_1, which involve the first two exact moments & the covariance of random variables x & y [3].

$$\mu_x = tr(\Sigma^2) + \frac{1}{N}(\mathrm{tr}(\Sigma))^2 \tag{4.49}$$

$$\mu_{xy} = \frac{2}{N} tr(\Sigma^3) + \frac{2}{N^2} \mathrm{tr}(\Sigma)\mathrm{tr}(\Sigma^2) \tag{4.50}$$

$$\mu_z \approx \frac{\mu_x}{{\mu_y}^2} - \frac{2\mu_{xy}}{{\mu_y}^3} + \frac{3\mu_x v_y}{{\mu_y}^4} \tag{4.51}$$

$$v_z = \frac{v_x}{{\mu_y}^4} - \frac{4\mu_x\mu_{xy}}{{\mu_y}^5} + \frac{4{\mu_x}^2 v_y}{{\mu_y}^6} \tag{4.52}$$

Where μ_{xy} is the covariance of x & y.

$$v_x = \frac{4}{N} tr(\Sigma^4) + \frac{2}{N^2}(4\mathrm{tr}(\Sigma)\mathrm{tr}(\Sigma^3) + (\mathrm{tr}(\Sigma^2))^2) + \frac{2}{N^3}(2(\mathrm{tr}(\Sigma))^2\mathrm{tr}(\Sigma^2) + tr(\Sigma^4)) \tag{4.53}$$

$$\mu_y = tr(\Sigma) \tag{4.54}$$

$$v_y = \frac{1}{N} tr(\Sigma^2) \tag{4.55}$$

With the estimates of the mean (4.51) & variance (4.52), closed-form distributions of T_{SJD} for H_1can be constructed [3]. Also select the Beta distribution in Appendix C eq. (4.89), thus it has the same support as T_{SJD}. I have distribution under H_1 holds the same form as the Proposition 5:

Proposition 5: For any sensor size K & sample size N, the Beta approximation to the CDF of T_{SJD} for H_1 derived on the estimated value of the two first moments in eq. (4.51) & (4.52), is equals [10];

$$F_{SJDP_D}(\mathrm{y}) \approx 1 - \frac{\beta_{\frac{K(1-y)}{K-1};\ \alpha_1,\ \beta_1)}}{\beta(\alpha_1,\ \beta_1)}, \quad \mathrm{y} \in [\frac{1}{k}, 1] \tag{4.56}$$

Where α_1 & β_1 are calculated as:

$$\boldsymbol{\alpha_1} = \frac{(1-K\mu_z)(\mu_z-1)(K\mu_z-1)+Kv_z}{(K-1)K\mu_z},\ \boldsymbol{\beta_1} = \frac{(\mu_z-1)(\mu_z-1)(K\mu_z-1)+Kv_z}{(K-1)\mu_z} \quad \textbf{(4.57)}$$

From the $T_{SJD}$for H_1(4.41) & Proposition 5, the P_D approximation is.

$$\boldsymbol{P_D(\Lambda) = 1 - F_{SJDP_D}(\Lambda)} \approx \frac{\beta_{\Lambda}(\frac{K(1-\Lambda)}{K-1}; \alpha_1, \beta_1)}{\beta(\alpha_1, \beta_1)} \quad \textbf{(4.58)}$$

The closed-form of approximative P_{FA} using eq. (4.56) & the P_D from eq. (4.58),

$$\boldsymbol{P_D = 1 - F_{SJDP_D}(F_{SJD}^{-1}(1 - P_{FA})} \quad \textbf{(4.59)}$$

The parameters a_0, β_0 in eq. (4.55) & a_1, β_1 in eq. (4.57) are only the elementary functions of the sensor size K, the sample size N & the population covariance matrix Σ. Therefore, P_D is depending on these parameters.

Selection Combining fusion in Rayleigh fading: For Rayleigh fading channel by assuming S-channels with average SNR of $\overline{\gamma}$ per-channel inserting the PDF & CDF [14] of the expression for combiner output SNR PDF is written as [15];

$$\boldsymbol{f_{R\gamma_{sc}}(\gamma_{sc}) = \frac{N}{\overline{\gamma}}[1 - \exp(-\frac{\gamma_{sc}}{\gamma_{sc}})]^{N-1} \times \exp(-\frac{\gamma_{sc}}{\gamma_{sc}}),\quad \gamma_{sc} \geq 0} \quad \textbf{(4.62)}$$

Using the relation [16 (4.13)];

$$\boldsymbol{[1 - \exp(-x)]^N = \sum_{k=0}^{N}\binom{N}{k}(-1)^k exp(-kx)} \quad \textbf{(4.63)}$$

In appropriate form of the $f_{R\gamma_{sc}}(\gamma_{sc})$ in (4.62) re-written as;

$$\boldsymbol{f_{R\gamma_{sc}}(\gamma_{sc}) = N\sum_{k=0}^{N-1}\frac{(-1)^k}{k+1}\binom{N-1}{k}\frac{1}{\overline{\gamma}/_{(k+1)}} \times exp(\frac{\gamma_{sc}}{\overline{\gamma}/_{(k+1)}}),\quad \gamma_{sc} \geq 0} \quad \textbf{(4.64)}$$

From eq.(4.64) can be calculate the probability of detection for the Spherical & John's detector under selection combining scheme with Rayleigh fading channel written as in eq.(4.65) & (4.66) respectively: By replacing the value of $f_{R\gamma_{sc}}(\gamma_{sc})$ from eq. (4.64) instead of $\frac{1}{\overline{\gamma}}e^{\frac{\gamma}{\overline{\gamma}}}$ to (4.61) can gives eq. (4.65).

$$\boldsymbol{\overline{P}_{D,\,sc,Ray} \approx N\sum_{k=0}^{N-1}\frac{(-1)^k}{k+1}\binom{N-1}{k}\frac{k+1}{\overline{\gamma}} \times \int_0^{\infty}\frac{(1-\Lambda)^{\beta_1}\sum_{j=\alpha_1}^{\infty}\binom{\beta_1+j-1}{j}\Lambda^j}{\sqrt{2\pi}\frac{\alpha_1^{\alpha_1-1/2}\beta_1^{\beta_1-1/2}}{(\alpha_1+\beta_1)^{\alpha_1+\beta_1-1/2}}}\exp(\frac{(k+1)\gamma_{sc}}{\overline{\gamma}})\,d\gamma_{sc}} \quad \textbf{(4.65)}$$

$$\overline{P}_{D,\,sc,Ray} \approx N \sum_{k=0}^{N-1} \frac{(-1)^k}{k+1} \binom{N-1}{k} \frac{k+1}{\overline{\gamma}} \times \int_0^{\infty} \frac{\int_0^{\frac{K(1-\Lambda)}{K-1}} \frac{K(1-\Lambda)}{K-1}^{\alpha_1-1} (1-\frac{K(1-\Lambda)}{K-1})^{\beta_1-1} d\Lambda}{\sqrt{2\pi} \frac{\alpha_1^{\alpha_1-1/2} \beta_1^{\beta_1-1/2}}{(\alpha_1+\beta_1)^{\alpha_1+\beta_1-1/2}}} \exp\left(\frac{(k+1)\gamma_{sc}}{\overline{\gamma}}\right) d\gamma_{sc} \quad (4.66)$$

3. Simulation Results & Discusions

In this section, the simulation results of MATLAB2013a based methods & interpretation of the results are included. The performance comparisons are analysed based on detection probability versus SNR, false alarm probability, & using ROC over Rayleigh fading channel for P≥ 1 PUs & more than two SUs which detect the primary signal cooperatively to check presence or absence of primary users. In addition to that the simulations are achieved by Monte Carlo method which uses for random signals in stochastic methods. The simulation parameters which uses for this work are listed below in Table 4.1.

Table 3.1: Simulation parameters

Simulation of Parameters	Values
Number of transmitter & receiver	≥2
Number of PUs	≥1
Number of SUs	[4, 6]
Transmission bandwidth	7Mhz
Center frequency	5MHz & 6MHz
Modulation	BPSK
Noise	White Gaussian
Channel	Rayleigh Fading channel
Number of samples	10,000
Number of Monte Carlo	100,000
SNR interval	[-20,0] dB
Cooperative network	Soft fusion-center with SC scheme
Detection Probability	1
False alarm Probability	≤0.1
Detector	Spherical & Johnson's

3.1 Comparison of Detection Performance on Different SNR Values

Figure 3.1 shows the relationship between the P_D & the SNR for a single licensed band detected by four SUs (CRUs).

The results of SD using GLRT gives the good detection performance which compared to JD using LBIT estimator. JD is greatly affected by interference as shown in Figure 3.1 due to its low detection performance.

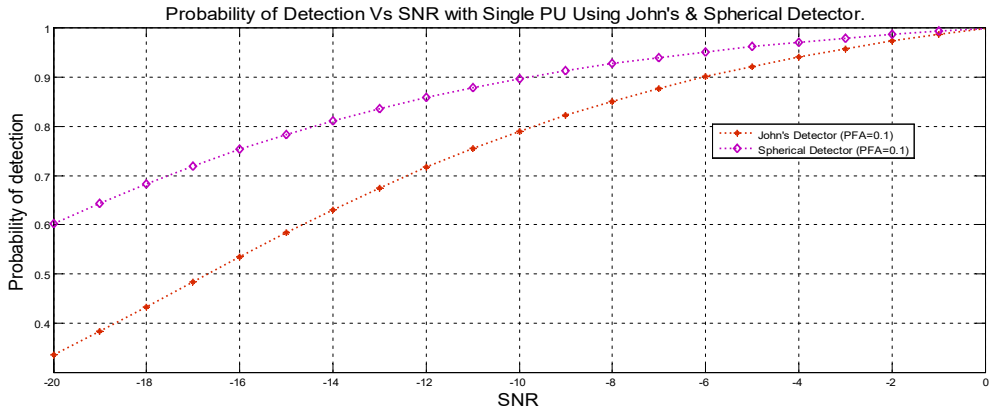

Figure 3.1: P_D Vs SNR in dB with PU=1, SU=4 & 0.1 P_{FA}.

The simulation result in Figure 3.2 Shown the detection of two PUs with four SUs. Then the P_D under JD started with the high improvements compared to single primary user that performance values of around 0.915. On the other hand, in the SD perform around 0.968 with the same SNR value. Generally, spectrum sensing by using these algorithms with two PUs has good performance improvements at the initially as compared to the single PUs.

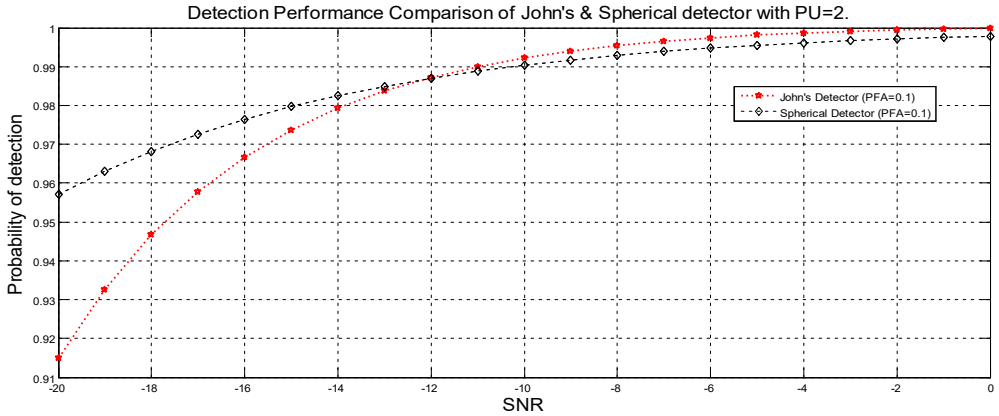

Figure 3.2: P_D Vs SNR in dB with PU=2, SU=4 & 0.1 P_{FA}.

3.2 Performance Change with Different Probability of False Alarm

The output curves presented in Figure 3.3 indicate the relationship between signal & noise in the receiver for SD & JD with two primary & six SUs. The detection probabilities are analysed based on 100,000 Monte Carlo sample values. In a SD when the P_{FA} increases from 0.05 to 0.1 obtain around 0.032 detection performance improvements. Generally, in case of JD shows the better performance improvement with increment of P_{FA} from 0.05 to 0.1.

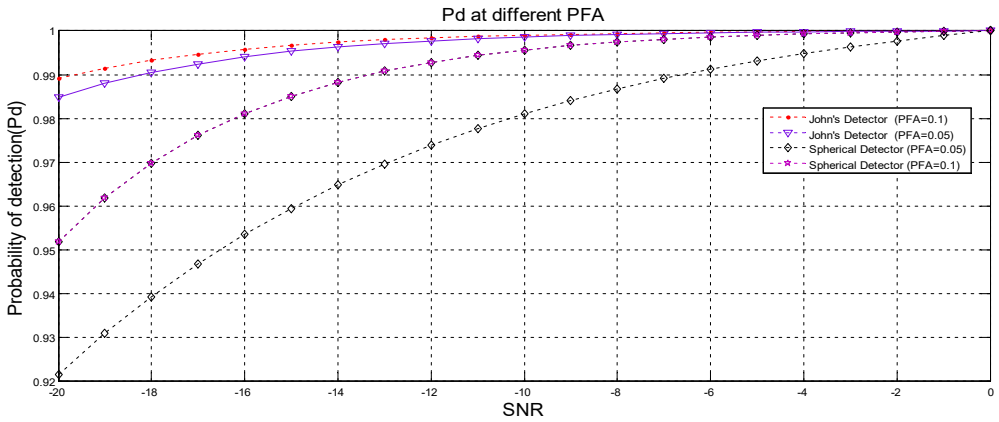

Figure 3.3: P_D with different P_{FA} using 2 PUs & 6 SUs.

3.3 Complementary ROC Curves of Spherical & John's Detector

The Figure 3.4 shows the ROC of JD with LBIT & SD with GLRT/MLRT estimator under constant values of PUs, SUs SNR. The SD gives the better detection performance & also achieved the required P_D at value of around 0.098 P_{FA}. However, in case of SD even if at 0.1 P_{FA} not achieved. Hence the estimation of the received PU signal with help of LBIT is better than GLRT/MLRT estimator in low SNR scenario for multiple PU detection.

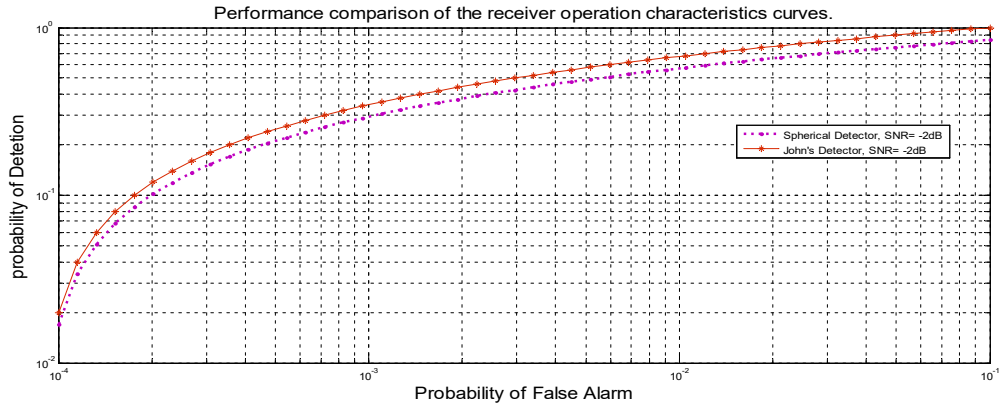

Figure 3.4: P_D Vs P_{FA} ROC with PU=2, SU=5 & at -2dB SNR.

3.4 Performance Comparison of John's Detector with Other Detector

As shown in the results of the above Figures generally JD provides the better detection performance in the presence of two PUs. In addition to this its performance is good when compared to the other detection method. For example, the comparison result shows in Figure 3.5 with Eigenvalue based detector at value of -20dB SNR & 0.1 P_{FA}. At these values of parameters JD & Eigenvalue based detector gives 96% & 88% P_D respectively. So JD achieved by 8% improvement.

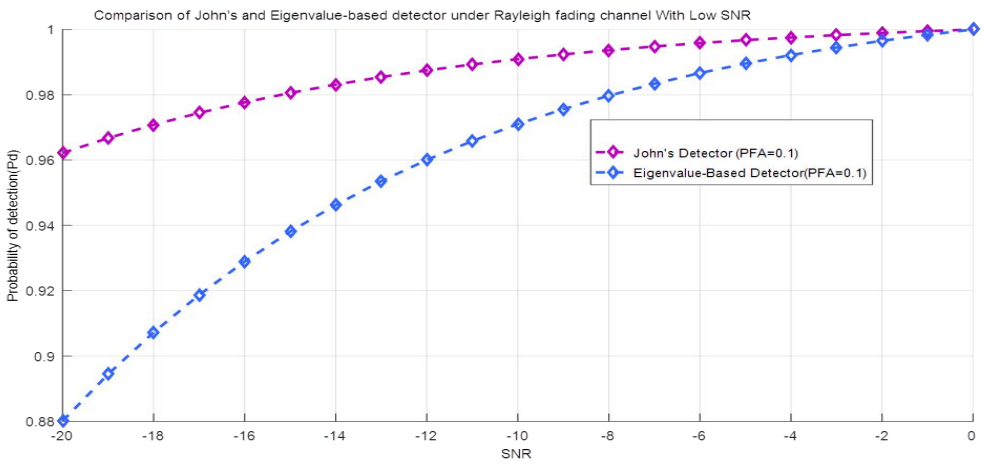

Figure 3.5 Performance Comparison of John's with Eigenvalue based detector P_D Vs SNR in the presence of PU=2, SUs=5 & P_{FA}= 0.1.

4. Conclusion & Future Works

The spectrum sensing using a single PU leads to analytically controllable problem & increases the traffic congestion. This research work investigates the comparative analysis of SD & JD schemes in the presence of a single & two PUs detected by four, five & six SUs in cooperative manner. The investigation is done under consideration of low SNR range. The detection of weak PU signal by SUs individually is a challenging task however this challenge can be mitigated by using cooperative mechanism.

The results of the experiment depicts that the performance of detecting a single PU by four SUs shows poor performance as compared to the two PUs. The next experiment investigates the effect of P_{FA} in fixed SNR ranges [-20, -2] for both JD & SD methods. The result of SD methods at P_{FA}value of 0.05 the detection ranges is between 92% and 99.8% & for the value of P_{FA} 0.1 the result ranges from 95% to 99.9%. In the case of JD method, the corresponding experiment of P_{FA}value of 0.05 gives performance of detection between 98.5% & 100%.

Future Works. This research done the theoretical & simulation based experimental analysis of JD & SD methods using single and two PUs. In the future,conduct the practical implementation of the system using the appropriate hardware and software systems.

References

[1] X. Yang et al.. (2018). *Threshold Setting for Multiple Primary User Spectrum Sensing via Spherical Detector* [Online]. Available: doi: 10.1109/LWC.2018.2877361

[2] Sattar J. et al. (2014). *Cognitive Spectrum Sensing with Multiple Primary Users in*

Rayleigh Fading Channels [Online]. Available: doi: 10.3390/electronics3030553

[3] L. Wei, P. Dharmawansa, and O. Tirkkonen, "Multiple Primary User Spectrum Sensing in the Low SNR Regime," *IEEE Trans. Commun*., Vol. 61, no. 5, pp. 1720-1731, 2013.

[4] X. Yang et al.. (2018). *Threshold Setting for Multiple Primary User Spectrum Sensing via Spherical Detector* [Online]. Available: doi: 10.1109/LWC.2018.2877361

[5] L. Wei, S. Member, and O. Tirkkonen, "Spectrum Sensing in the Presence of Multiple Primary Users," *IEEE Trans., On Commun.*, pp. 1–23, 2012.

[6] *An introduction to multivariate statistical analysis,* N. York, Wiley, 1958, pp. 5-3.

[7] M. Mourad and A. Hussein, "Major Spectrum Sensing Techniques for Cognitive Radio Networks: A Survey," *Int. J. Eng. Innovation Technology*, Vol. 5, no. 3, pp. 24-37, 2015.

[8] N. Sugiura, "LBIT for Sphericity and Limiting Distributions," *The Ann. of Math. Statistics*, Vol. 43, no. 4, pp. 1312–1316, 1972.

[9] M. Pesavento, A. M. Zoubir, and S. J. Detection, Decentralized Cooperative Detection Based on Averaging Consensus, July 2016.

[10] C. Stevenson et al., *IEEE 802.22*: *The First Cognitive Radio Wireless Regional Area Network Standard*, Commun. Mag., IEEE, 2009.

[11] N. Sugiura, "Locally Best Invariant Test for Sphericity and the Limiting Distributions," *the Ann. of Math. Stat.*, Vol. 43, no.4, pp. 1312-1316, Aug. 1972.

[12] S. John,"The Distribution of a Statistic Used for Testing Sphericity of Normal Distributions," *Biometrika*, Vol. 59, no. 1, pp. 169-173, Apr. 1972.

[13] L. Wei, P. Dharmawansa and O. Tirkkonen. (2012, March). *Locally Best Invariant Test for Multiple Primary User Spectrum Sensing* [Online]. Available: doi:10.4108/ics.crowncom.2012. 248444

[14] S. Nallagonda, et al., "Detection Performance of Soft Data Fusion in Rician Fading Channel for Cognitive Radio Network," *Proc. of Int. Symp. on Wireless Personal Multimedia Commun. (WPMC'15)*, pp. 1-5, 2015.

[15] M. S. Sumi and R. S. Ganesh. (2019). *Improved EGC Method for Increasing Detection in Cognitive Radio Networks* [Online]. Available: doi: 10.1016/j.comcom.2019.08.019

[16] A. Chandra, "Performance Analysis of Diversity Combining Techniques for Digital Signals in Wireless Fading Channels," Ph.D. Thesis, Jadavpur Univ., Kolkata, India, 2011.